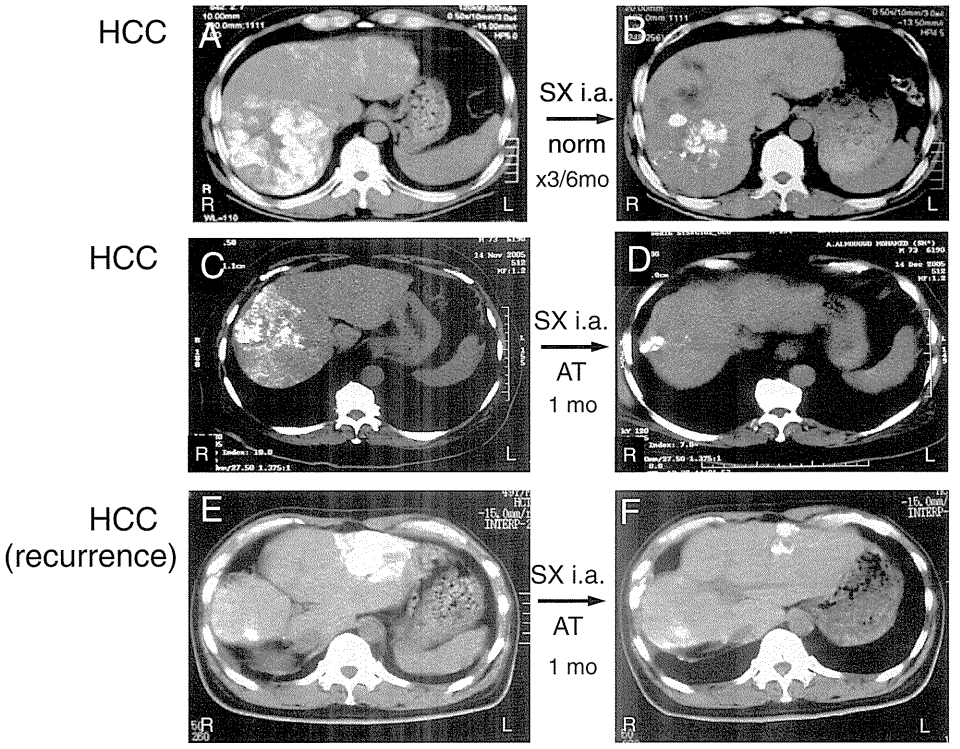

Fig. 10. CT scan images of primary and recurrent hepatocellular carcinoma (HCC). Patient on the top with massive primary liver cancer received about 5–6 mg SMANCS(SX)/5–6 mL Lipiodol(LP) (A). Subsequently, the patient received three injections of the drug i.a. under normotensive state in 6 mon, then marked regression was obtained (→ B). CT scans in (C) and (E) patients received i.a. infusion of SX/LP under hypertension induced by intravenous infusion of AT-II. In about 1 mon, the size of tumors in both cases was reduced to less than 10% of the original size (Fig. 10 C → D; E → F) (adapted from ref. 88)).

effects in healthy people and are active only in hypertensive patients and more selectively at tumor sites in this case. Data indicate that ACE inhibitors, such as enalapril increased drug delivery about 2- to 3-fold (Fig. 13).[99),100)] Professor Felix Kratz also confirmed this effect in different tumor models with different polymeric drugs (personal communication).

We likewise found that beraprost sodium, a stable analogue (prolonged plasma $t_{1/2}$, 30 times) of prostaglandin I_2, which administered orally, enhanced tumor-targeted drug delivery in mouse tumors.[78)]

7. Concluding remarks

Tumor vasculature is structurally unique and different from normal vasculature. Tumor tissue also shows highly up-regulated production of vascular effectors. As a consequence extravasation of macromolecules into the interstitial space would occur. The effectors affecting vascular permeability factors includes (brady)kinin, NO, prostaglandins, VEGF (or vascular permeability factor), and CO (by HO-1) in or near the most solid tumors. This enhanced vascular permeability also commonly occurs in inflamed tissue at the sites of infection that is affected by many similar vascular mediators.

Once macromolecules extravasate from the circulation or blood vessels into the tumor interstitium, they remain in the tumor for a long time without being cleared. This situation is in great contrast to normal tissue, in which macromolecules are cleared via the lymphatic system. Thus, prolonged retention of macromolecules—for more than days to weeks—is a unique characteristic of the EPR effect in tumor tissue. These features led to this phenomenon being named the *enhanced permeability and retention (EPR) effect* of macromolecules in solid tumor.[26)–32),35),36)] The EPR effect is applicable to biocompatible macromolecules with MW > 40 KDa.

However, the EPR effect occurs frequently heterogeneously, which means that tumor selective macromolecular drug delivery based on the EPR effect may not procede homogeneously. Consequently, drug delivery may be less efficient to

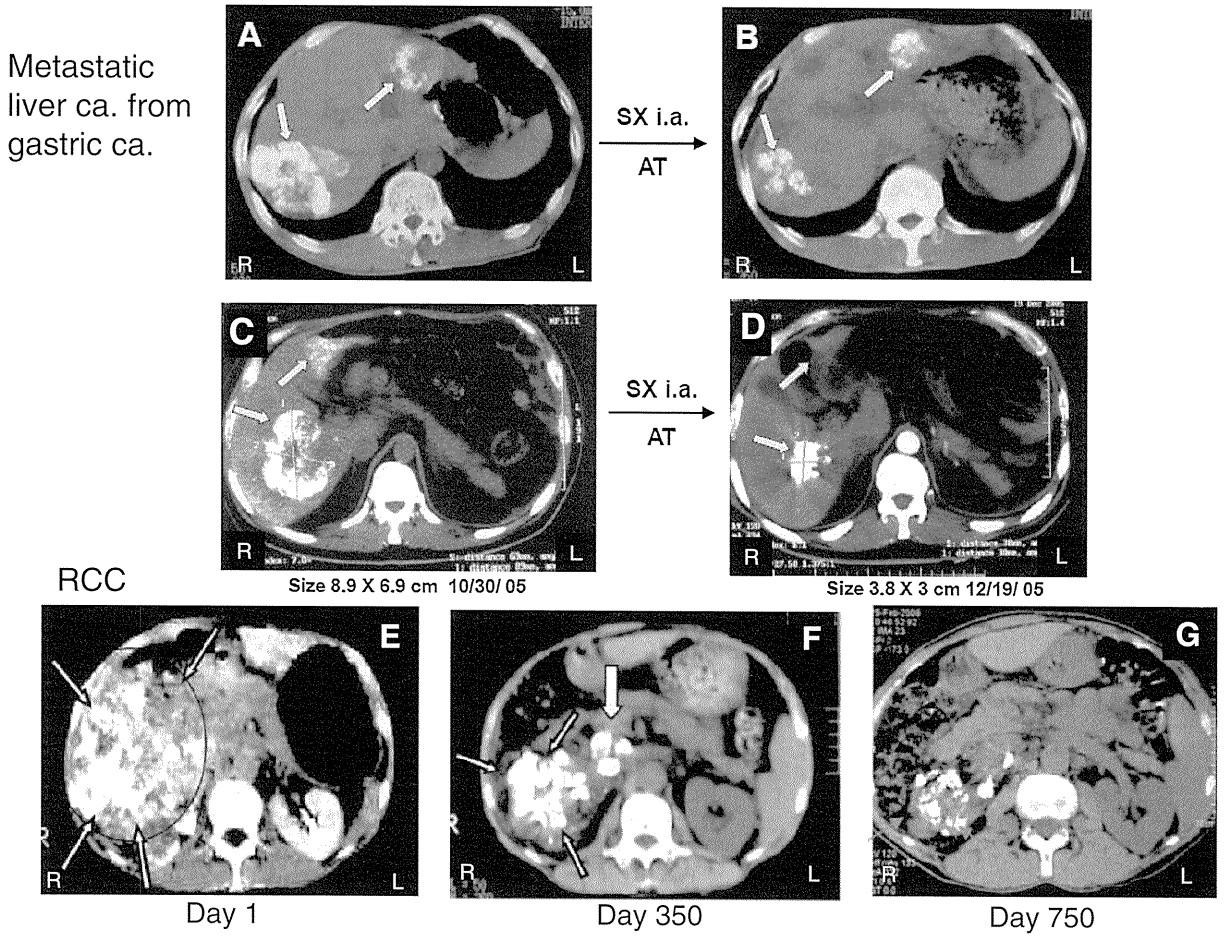

Fig. 11. CT scan images of (A) and (C) show stomach cancer metastasized to the liver. They received SX/LP(SMANCS/Lipiodol) i.a. under AT-II-induced hypertension, at about 150–160 mmHg. The notable reduction to about 10% of the original volume of tumor was observed in 1–2 months (see B,D) (Adapted from ref. 88)). In the bottom three CT images showing a case of massive renal carcinoma. SX/LP was administered via the renal artery under AT-II-induced hypertension. CT scans at left was taken at day 1, middle at day 350, and on lower right at day 750 showing remarkable regression. Also please note a metastatic tumor nodule at the inferior vena cava (middle; large white arrow). This metastatic tumor (nodule) regressed to a small spot in the scan at day 750 (right). Dose of SX/LP administration was 3–4 mg in about 2 ml at a time, and the patient received total of 14 times i.a. infusion in three years. This patient is still alive after 9 years with good QOL.

metastatic liver cancers and to less vascularized cancers, *e.g.*, cancers of the pancreas and prostate, rendering poor EPR effect. Therefore better therapeutic outcomes for such cancers depends on further augmentation of drug delivery to such tumors. We thus developed measures to enhance the EPR effect. One method involves raising the systemic blood pressure, *e.g.*, from 100 to 160 mmHg by using angiotensin II during arterial infusion of a macromolecular drug, *e.g.*, SMANCS/Lipiodol. This method produced excellent clinical results even in advanced and difficult-to-treat tumors such as metastatic liver cancer, cholangiocarcinoma, and cancers of the pancreas, and others.[88]

Another method is utilization of NO-releasing agents such as NG for advanced and poor-EPR tumors. Hypoxic tumor tissues and infarcted cardiac tissue (as in angina pectoris) seem to possess similar NO-related mechanisms. Topical application of NG results the site-selective increase of NO concentration, which did facilitate an improved EPR effect[89),90)] and clinical benefit.[94)–98)] Similarly, ACE inhibitors can increase the local kinin concentration, and thus enhanced EPR effect without any adverse effects.[99),100)] These methods of enhancing the EPR effect will likely achieve better clinical outcomes for cancer patients without any adverse effects and warrant continuing development.

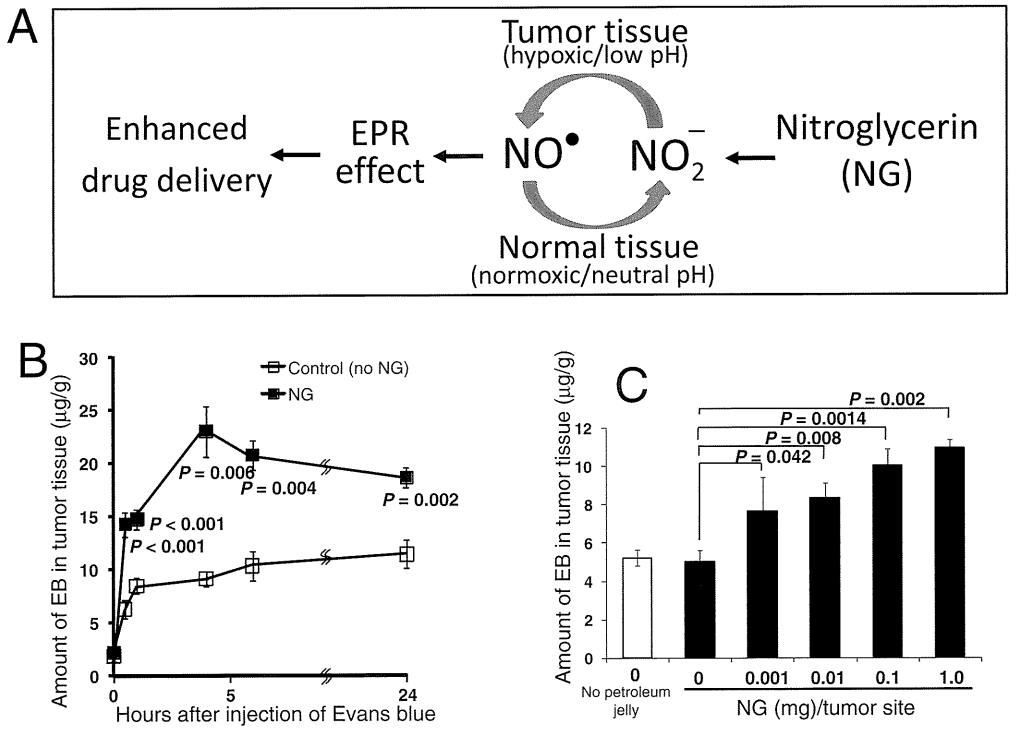

Fig. 12. (A) Mechanism of NO generation and enhancement of the EPR effect by topical application of NO-releasing agent, nitroglycerin (NG). NG will get into circulation in a few min, and NO_2^- is liberated, and in the hypoxic tumor tissue NO_2^- is reduced to nitric oxide (NO) which induces the vascular permeability. Time course (B) and dose dependence (C) of NG-induced augmentation of EPR effect in S-180 tumors were probed with Evans blue/albumin accumulation in tumor. Chemically induced rat tumor with (DMBA) and other tumors (Meth A fibrosarcoma and colon 38 adenocarcinoma) also showed similar results (Adapted from ref. 89)).

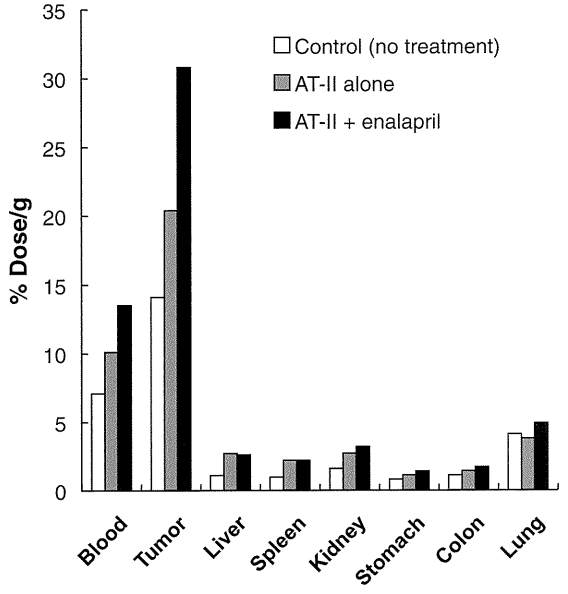

Fig. 13. Augmentation of EPR effect and macromolecular drug delivery to tumor by using AT-II and ACE inhibitor enalapril. The drug used here was monoclonal antibody A7 against human colon cancer in athymic mice bearing SW-1116 tumor cells. IgG was labeled with ^{125}I (Adapted from ref. 99)).

Acknowledgements

I would like to acknowledge invaluable contributions and collaborations or support of all the colleagues whose names are either referred in the text or references, Asami Takaki, and Judith Gandy for the preparation of manuscript. Research grants from the MEXT and MHLW of Japanese Government, and BioDynamics Research Foundation of Kumamoto for sustained support for over many years.

References

1) Matsumoto, K., Yamamoto, T., Kamata, R. and Maeda, H. (1984) Pathogenesis of serratial infection: activation of the Hageman factor-prekallikrein cascade by serratial protease. J. Biochem. **96**, 739–749.
2) Kamata, R., Yamamoto, T., Matsumoto, K. and Maeda, H. (1985) A serratial protease causes vascular permeability reaction by activation of the Hageman factor-dependent pathway in guinea pigs. Infect. Immun. **48**, 747–753.
3) Molla, A., Yamamoto, T., Akaike, T., Miyoshi, S. and Maeda, H. (1989) Activation of Hageman

factor and prekallikrein and generation of kinin by various microbial proteinases. J. Biol. Chem. **264**, 10589–10594.
4) Maruo, K., Akaike, T., Inada, Y., Ohkubo, I., Ono, T. and Maeda, H. (1993) Effect of microbial and mite proteases on low and high molecular weight kininogens. J. Biol. Chem. **268**, 17711–17715.
5) Maeda, H. (2002) Microbial proteinases and pathogenesis of infection. *In* The Encyclopedia of Molecular Medicine, vol. 4 (ed. Creighton, T.E.). John Wiley & Sons, New York, pp. 2663–2668.
6) Maeda, H. (1996) Role of microbial proteases in pathogenesis. Microbiol. Immunol. **40**, 685–699.
7) Maeda, H., Matsumura, Y. and Kato, H. (1988) Purification and identification of [hydroxyprolyl^3]-bradykinin in ascitic fluid from a patient with gastric cancer. J. Biol. Chem. **263**, 16051–16054.
8) Matsumura, Y., Kimura, M., Yamamoto, T. and Maeda, H. (1988) Involvement of the kinin-generating cascade and enhanced vascular permeability in tumor tissue. Jpn. J. Cancer Res. **79**, 1327–1334.
9) Matsumura, Y., Maruo, K., Kimura, M., Yamamoto, T., Konno, T. and Maeda, H. (1991) Kinin-generating cascade in advanced cancer patients and *in vitro* study. Jpn. J. Cancer Res. **82**, 732–741.
10) Maeda, H., Wu, J., Okamoto, T., Maruo, K. and Akaike, T. (1999) Kallikrein-kinin in infection and cancer. Immunopharmacology **43**, 115–128.
11) Maeda, H., Noguchi, Y., Sato, K. and Akaike, T. (1994) Enhanced vascular permeability in solid tumor is mediated by nitric oxide and inhibited by both new nitric oxide scavenger and nitric oxide synthase inhibitor. Jpn. J. Cancer Res. **85**, 331–334.
12) Wu, J., Akaike, T., Hayashida, K., Okamoto, T., Okuyama, A. and Maeda, H. (2001) Enhanced vascular permeability in solid tumor involving peroxynitrite and matrix metalloproteinase. Jpn. J. Cancer Res. **92**, 439–451.
13) Wu, J., Akaike, T. and Maeda, H. (1998) Modulation of enhanced vascular permeability in tumors by a bradykinin antagonist, a cyclooxygenase inhibitor, and a nitric oxide scavenger. Cancer Res. **58**, 159–165.
14) Okamoto, T., Akaike, T., Nagano, T., Miyajima, S., Suga, M., Ando, M., Ichimori, K. and Maeda, H. (1997) Activation of human neutrophil procollagenase by nitrogen dioxide and peroxynitrite: a novel mechanism for procollagenase activation involving nitric oxide. Arch. Biochem. Biophys. **342**, 261–274.
15) Maeda, H., Fang, J., Inutsuka, T. and Kitamoto, Y. (2003) Vascular permeability enhancement in solid tumor: various factors, mechanisms involved and its implications. Int. Immunopharmacol. **3**, 319–328.
16) Maeda, H., Akaike, T., Wu, J., Noguchi, Y. and Sakata, Y. (1996) Bradykinin and nitric oxide in infectious disease and cancer. Immunopharmacology **33**, 222–230.
17) Maeda, H., Takeshita, J. and Kanamaru, R. (1979) A lipophilic derivative of neocarzinostatin: A polymer conjugation of an antitumor protein antibiotic. Int. J. Pept. Protein Res. **14**, 81–87.
18) Maeda, H., Ueda, M., Morinaga, T. and Matsumoto, T. (1985) Conjugation of poly(styrene-co-maleic acid) derivatives to the antitumor protein neocarzinostatin: Pronounced improvements in pharmacological properties. J. Med. Chem. **28**, 455–461.
19) Iwai, K., Maeda, H. and Konno, T. (1984) Use of oily contrast medium for selective drug targeting to tumor: enhanced therapeutic effect and X-ray image. Cancer Res. **44**, 2115–2121.
20) Iwai, K., Maeda, H., Konno, T., Matsumura, Y., Yamashita, R., Yamasaki, K., Hirayama, S. and Miyauchi, Y. (1987) Tumor targeting by arterial administration of lipids: rabbit model with VX2 carcinoma in the liver. Anticancer Res. **7**, 321–328.
21) Courtice, F.C. (1996) The origin of lipoproteins in lymph. *In* Lymph and Lymphatic System (ed. Mayerson). Charles C Thomas Publisher, Springfield, IL, pp. 89–126.
22) Maeda, H., Takeshita, J. and Yamashita, A. (1980) Lymphotropic accumulation of an antitumor antibiotic protein, neocarzinostatin. Eur. J. Cancer **16**, 723–731.
23) Takeshita, J., Maeda, H. and Kanamaru, R. (1982) *In vitro* mode of action, pharmacokinetics, and organ specificity of poly (maleic acid-styrene)-conjugated neocarzinostatin, SMANCS. Gann **73**, 278–284.
24) Konno, T., Maeda, H., Iwai, K., Tashiro, S., Maki, S., Morinaga, T., Mochinaga, M., Hiraoka, T. and Yokoyama, I. (1983) Effect of arterial administration of high-molecular-weight anticancer agent SMANCS with lipid lymphographic agent on hepatoma: a preliminary report. Eur. J. Cancer Clin. Oncol. **19**, 1053–1065.
25) Konno, T., Maeda, H., Iwai, K., Maki, S., Tashiro, S., Uchida, M. and Miyauchi, Y. (1984) Selective targeting of anticancer drug and simultaneous image enhancement in solid tumors by arterially administered lipid contrast medium. Cancer **54**, 2367–2374.
26) Maki, S., Konno, T. and Maeda, H. (1985) Image enhancement in computerized tomography for sensitive diagnosis of liver cancer and semiquantitation of tumor selective drug targeting with oily contrast medium. Cancer **56**, 751–757.
27) Matsumura, Y. and Maeda, H. (1986) A new concept for macromolecular therapeutics in cancer chemotherapy: mechanism of tumoritropic accumulation of proteins and the antitumor agent SMANCS. Cancer Res. **46**, 6387–6392.
28) Noguchi, Y., Wu, J., Duncan, R., Strohalm, J., Ulbrich, K., Akaike, T. and Maeda, H. (1998) Early phase tumor accumulation of macromolecules: a great difference in clearance rate between tumor and normal tissues. Jpn. J. Cancer Res. **89**, 307–314.

29) Seymour, L.W., Miyamoto, Y., Maeda, H., Brereton, M., Strohalm, J., Ulbrich, K. and Duncan, R. (1995) Influence of molecular weight on passive tumour accumulation of a soluble macromolecular drug carrier. Eur. J. Cancer **31**, 766–770.
30) Maeda, H., Wu, J., Sawa, T., Matsumura, Y. and Hori, K. (2000) Tumor vascular permeability and the EPR effect in macromolecular therapeutics. J. Control. Release **65**, 271–284.
31) Maeda, H., Sawa, T. and Konno, T. (2001) Mechanism of tumor-targeted delivery of macromolecular drugs, including the EPR effect in solid tumor and clinical overview of the prototype polymeric drug SMANCS. J. Control. Release **74**, 47–61.
32) Maeda, H. (2001) The enhanced permeability and retention (EPR) effect in tumor vasculature: the key role of tumor-selective macromolecular drug targeting. Adv. Enzyme Regul. **41**, 189–207.
33) Maeda, H. and Matsumura, Y. (1989) Tumoritropic and lymphotropic principles of macromolecular drugs. Crit. Rev. Ther. Drug Carrier Syst. **6**, 193–210.
34) Maeda, H., Bharate, G.Y. and Daruwalla, J. (2009) Polymeric drugs and nanomedicines for efficient tumor targeted drug delivery based on EPR-effect. Eur. J. Pharm. Biopharm. **71**, 409–419.
35) Maeda, H. (2010) Tumor-selective delivery of macromolecular drugs via the EPR effect: background and future prospects. Bioconjug. Chem. **21**, 797–802.
36) Maeda, H. (2011) The EPR-effect in relation to tumor targeting. *In* Drug Delivery in Oncology. From Basic Research to Cancer Therapy (eds. Kratz, F., Senter, P. and Steinhagen, H.). Wiley-VCH Verlag GmbH & Co. KG, Weinheim, Germany, pp. 65–86.
37) Kimura, N., Taniguchi, S., Aoki, K. and Baba, T. (1980) Selective localization and growth of *Bifidobacterium bifidum* in mouse tumors following intravenous administration. Cancer Res. **40**, 2061–2068.
38) Zhao, M., Yang, M., Li, X.M., Jiang, P., Baranov, E., Li, S., Xu, M., Penman, S. and Hoffman, R.M. (2005) Tumor-targeting bacterial therapy with amino acid auxotrophs of GFP-expressing *Salmonella typhimurium*. Proc. Natl. Acad. Sci. U.S.A. **102**, 755–760.
39) Hoffman, R.M. (2009) Tumor-targeting amino acid auxotrophic *Salmonella typhimurium*. Amino Acids **37**, 509–521.
40) Konerding, M.A., Miodonski, A.J. and Lametschwandtner, A. (1995) Microvascular corrosion casting in the study of tumor vascularity: a review. Scanning Microsc. **9**, 1233–1244.
41) Hashizume, H., Baluk, P., Morikawa, S., McLean, J.W., Thurston, G., Roberge, S., Jain, R.K. and McDonald, D.M. (2000) Openings between defective endothelial cells explain tumor vessel leakiness. Am. J. Pathol. **1561**, 1363–1380.
42) Skinner, S.A., Tutton, P.J. and O'Brien, P.E. (1990) Microvascular architecture of experimental colon tumors in the rat. Cancer Res. **50**, 2411–2417.
43) Malcontenti-Wilson, C., Muralidharan, V., Skinner, S., Christophi, C., Sherris, D. and O'Brien, P.E. (2001) Combretastatin A4 prodrug study of effect on the growth and the microvasculature of colorectal liver metastases in a murine model. Clin. Cancer Res. **7**, 1052–1060.
44) Daruwalla, J., Nikfarjam, M., Greish, K., Malcontenti-Wilson, C., Muralidharan, V., Christophi, C. and Maeda, H. (2010) *In vitro* and *in vivo* evaluation of tumor targeting styrene-maleic acid-pirarubicin micelles: survival improvement and inhibition of liver metastases. Cancer Sci. **101**, 1866–1874.
45) Folkman, J. (1971) Tumor angiogenesis: therapeutic implications. N. Engl. J. Med. **285**, 1182–1186.
46) Folkman, J. (1990) What is the evidence that tumors are angiogenesis dependent? J. Natl. Cancer Inst. **82**, 4–6.
47) Folkman, J. (1995) Angiogenesis in cancer, vascular, rheumatoid and other disease. Nat. Med. **1**, 27–31.
48) Senger, D.R., Galli, S.J., Dvorak, A.M., Perruzzi, C.A., Harvey, V.S. and Dvorak, H.F. (1983) Tumor cells secrete a vascular permeability factor that promotes accumulation of ascites fluid. Science **219**, 983–985.
49) Dvorak, H.F., Nagy, J.A., Dvorak, J.T. and Dvorak, A.M. (1988) Identification and characterization of the blood vessels of solid tumors that are leaky to circulating macromolecules. Am. J. Pathol. **133**, 95–109.
50) Dvorak, H.F., Brown, L.F., Detmar, M. and Dvorak, A.M. (1995) Vascular permeability factor/vascular endothelial growth factor, microvascular hyperpermeability, and angiogenesis. Am. J. Pathol. **146**, 1029–1039.
51) Leung, D.W., Cachianes, G., Kuang, W.J., Goeddel, D.V. and Ferrara, N. (1989) Vascular endothelial growth factor is a secreted angiogenic mitogen. Science **246**, 1306–1309.
52) Miller, J.W., Adamis, A.P., Shima, D.T., D'Amore, P.A., Moulton, R.S., O'Reilly, M.S., Folkman, J., Dvorak, H.F., Brown, L.F., Berse, B., Yeo, T.K. and Yeo, K.T. (1994) Vascular endothelial growth factor/vascular permeability factor is temporally and spatially correlated with ocular angiogenesis in a primate model. Am. J. Pathol. **145**, 574–584.
53) Dvorak, H.F., Nagy, J.A., Feng, D., Brown, L.F. and Dvorak, A.M. (1999) Vascular permeability factor/vascular endothelial growth factor and the significance of microvascular hyperpermeability in angiogenesis. Curr. Top. Microbiol. Immunol. **237**, 97–132.
54) Oda, T., Akaike, T., Hamamoto, T., Suzuki, F., Hirano, T. and Maeda, H. (1989) Oxygen radicals in influenza-induced pathogenesis and treatment with pyran polymer-conjugated SOD. Science **244**, 974–976.
55) Akaike, T., Ando, M., Oda, T., Doi, T., Ijiri, S.,

Araki, S. and Maeda, H. (1990) Dependence on O_2^- generation by xanthine oxidase of pathogenesis of influenza virus infection in mice. J. Clin. Invest. **85**, 739–745.
56) Maeda, H. and Akaike, T. (1991) Oxygen free radicals as pathogenic molecules in viral diseases. Proc. Soc. Exp. Biol. Med. **198**, 721–727.
57) Akaike, T., Noguchi, Y., Ijiri, S., Setoguchi, K., Suga, M., Zheng, Y.M., Dietzschold, B. and Maeda, H. (1996) Pathogenesis of influenza virus-induced pneumonia: involvement of both nitric oxide and oxygen radicals. Proc. Natl. Acad. Sci. U.S.A. **93**, 2448–2453.
58) Akaike, T., Fujii, S., Kato, A., Yoshitake, J., Miyamoto, Y., Sawa, T., Okamoto, S., Suga, M., Asakawa, M., Nagai, Y. and Maeda, H. (2000) Viral mutation accelerated by nitric oxide production during infection *in vivo*. FASEB J. **14**, 1447–1454.
59) Akaike, T. and Maeda, H. (2000) Pathophysiological effects of high-output production of nitric oxide. *In* Nitric Oxide (ed. Ignarro, L.J.). Academic Press, San Diego, pp. 733–745.
60) Akaike, T., Suga, M. and Maeda, H. (1998) Free radicals in viral pathogenesis: molecular mechanisms involving superoxide and NO. Proc. Soc. Exp. Biol. Med. **217**, 64–73.
61) Umezawa, K., Akaike, T., Fujii, S., Suga, M., Setoguchi, K., Ozawa, A. and Maeda, H. (1997) Induction of nitric oxide synthesis and xanthine oxidase and their role in the antimicrobial mechanism against *Salmonella typhimurium* in mice. Infect. Immun. **65**, 2932–2940.
62) Yoshitake, J., Akaike, T., Akuta, T., Tamura, F., Ogura, T., Esumi, H. and Maeda, H. (2004) Nitric oxide as an endogenous mutagen for Sendai virus without antiviral activity. J. Virol. **78**, 8709–8719.
63) Doi, K., Akaike, T., Horie, H., Noguchi, Y., Fujii, S., Beppu, T., Ogawa, M. and Maeda, H. (1996) Excessive production of nitric oxide in rat solid tumor and its implication in rapid tumor growth. Cancer **77**, 1598–1604.
64) Kuwahara, H., Kanazawa, A., Wakamatsu, D., Morimura, S., Kida, K., Akaike, T. and Maeda, H. (2004) Antioxidative and antimutagenic activities of 4-vinyl-2,6-dimethoxyphenol (canolol) isolated from canola oil. J. Agric. Food Chem. **52**, 4380–4387.
65) Kuwahara, H., Kariu, T., Fang, J. and Maeda, H. (2009) Generation of drug-resistant mutants of *Helicobacter pylori* in the presence of peroxynitrite, a derivative of nitric oxide at pathophysiological concentration. Microbiol. Immunol. **53**, 1–7.
66) Sawa, T. and Oshima, H. (2006) Nitrative DNA damage in inflammation and its possible role in carcinogenesis. Nitric Oxide **14**, 91–100.
67) Niles, J.C., Wishnok, J.S. and Tannenbaum, S.R. (2006) Peroxynitrite-induced oxidation and nitration products of guanine and 8-oxoguanine: structures and mechanisms of product formation. Nitric Oxide **14**, 109–121.
68) Maeda, H., Sawa, T., Yubisui, T. and Akaike, T. (1999) Free radical generation from heterocyclic amines by cytochrome b_5 reductase in the presence of NADH. Cancer Lett. **143**, 117–121.
69) Sjöblom, T., Jones, S., Wood, L., Parsons, D.W., Lin, J., Barber, T.D., Mandelker, D., Leary, R.J., Ptak, J., Silliman, N., Szabo, S., Buckhaults, P., Farrell, C., Meeh, P., Markowitz, S.D., Willis, J., Dawson, D., Willson, J.K.V., Gazdar, A.F., Hartigan, J., Wu, L., Liu, C., Parmigiani, G., Park, B.H., Bachman, K.E., Papadopoulos, N., Vogelstein, B., Kinzler, K.W. and Velculescu, V.E. (2006) The consensus coding sequences of human breast and colorectal cancers. Science **314**, 268–274.
70) Wood, L.D., Parsons, D.W., Jones, S., Lin, J., Sjöblom, T., Leary, R.J., Shen, D., Boca, S.M., Barber, T., Ptak, J., Silliman, N., Szabo, S., Dezso, Z., Ustyanksky, V., Nikolskaya, T., Nikolsky, Y., Karchin, R., Wilson, P.A., Kaminker, J.S., Zhang, Z., Croshaw, R., Willis, J., Dawson, D., Shipitsin, M., Willson, J.K.V., Sukumar, S., Polyak, K., Park, B.H., Pethiyagoda, C.L., Pant, P.V.K., Ballinger, D.G., Sparks, A.B., Hartigan, J., Smith, D.R., Suh, E., Papadopoulos, N., Buckhaults, P., Markowitz, S.D., Parmigiani, G., Kinzler, K.W., Velculescu, V.E. and Vogelstein, B. (2007) The genomic landscapes of human breast and colorectal cancers. Science **318**, 1108–1113.
71) Shah, S.P., Morin, R.D., Khattra, J., Prentice, L., Pugh, T., Burleigh, A., Delaney, A., Gelmon, K., Guliany, R., Senz, J., Steidl, C., Holt, R.A., Jones, S., Sun, M., Leung, G., Moore, R., Severson, T., Taylor, G.A., Teschendorff, A.E., Tse, K., Turashvili, G., Varhol, R., Warren, R.L., Watson, P., Zhao, Y., Caldas, C., Huntsman, D., Hirst, M., Marra, M.A. and Aparicio, S. (2009) Mutational evolution in a lobular breast tumour profiled at single nucleotide resolution. Nature **461**, 809–813.
72) Fojo, T. and Grady, C. (2009) How much is life worth: cetuximab, non–small cell lung cancer, and the $440 billion question. J. Natl. Cancer Inst. **101**, 1044–1048.
73) Mayer, R. (2009) Targeted therapy for advanced colorectal cancer—more is not always better. N. Engl. J. Med. **360**, 623–625.
74) Anonymous (2008) Welcome clinical leadership at NICE. Lancet **372**, 601.
75) Tol, J., Koopman, M., Cats, A., Rodenburg, C.J., Creemers, G.J.M., Schrama, J.G., Erdkamp, F.L.G., Vos, A.H., van Groeningen, C.J., Sinnige, H.A.M., Richel, D.J., Voest, E.E., Dijkstra, J.R., Vink-Börger, M.E., Antonini, N.F., Mol, L., van Krieken, J.H.J.M., Dalesio, O. and Punt, C.J.A. (2009) Chemotherapy, bevacizumab, and cetuximab in metastatic colorectal cancer. N. Engl. J. Med. **360**, 563–572.
76) Kano, M.R., Bae, Y., Iwata, C., Morishita, Y., Yashiro, M., Oka, M., Fujii, T., Komuro, A.,

Kiyono, K., Kaminishi, M., Hirakawa, K., Ouchi, Y., Nishiyama, N., Kataoka, K. and Miyazono, K. (2007) Improvement of cancer-targeting therapy, using nanocarriers for intractable solid tumors by inhibition of TGF-β signaling. Proc. Natl. Acad. Sci. U.S.A. **104**, 3460–3465.

77) Huang, S., Robinson, J.B., Deguzman, A., Bucana, C.D. and Fidler, I.J. (2000) Blockade of nuclear factor-κB signaling inhibits angiogenesis and tumorigenicity of human ovarian cancer cells by suppressing expression of vascular endothelial growth factor and interleukin 8. Cancer Res. **60**, 5334–5339.

78) Tanaka, S., Akaike, T., Wu, J., Fang, J., Sawa, T., Ogawa, M., Beppu, T. and Maeda, H. (2003) Modulation of tumor-selective vascular blood flow and extravasation by the stable prostaglandin I_2 analogue beraprost sodium. J. Drug Target. **11**, 45–52.

79) Doi, K., Akaike, T., Fujii, S., Tanaka, S., Ikebe, N., Beppu, T., Shibahara, S., Ogawa, M. and Maeda, H. (1999) Induction of haem oxygenase-1 by nitric oxide and ischaemia in experimental solid tumours and implications for tumour growth. Br. J. Cancer **80**, 1945–1954.

80) Fang, J., Qin, H., Nakamura, H., Tsukigawa, K. and Maeda, H. (2012) Carbon monoxide, generated by heme oxygenase-1, mediates the enhanced permeability and retention (EPR) effect of solid tumor. Cancer Sci. **103** (in press available online, Jan. 2012).

81) Sahoo, S.K., Sawa, T., Fang, J., Tanaka, S., Miyamoto, Y., Akaike, T. and Maeda, H. (2002) Pegylated zinc protoporphyrin: a water-soluble heme oxygenase inhibitor with tumor-targeting capacity. Bioconjug. Chem. **13**, 1031–1038.

82) Fang, J., Sawa, T., Akaike, T., Akuta, T., Greish, K., Hamada, A. and Maeda, H. (2003) *In vivo* antitumor activity of pegylated zinc protoporphyrin: targeted inhibition of heme oxygenase in solid tumor. Cancer Res. **63**, 3567–3574.

83) Fang, J., Akaike, T. and Maeda, H. (2004) Anti-apoptotic role of heme oxygenase and its potential as an anticancer target. Apoptosis **9**, 27–35.

84) Daruwalla, J., Greish, K., Wilson, C.M., Muralidharan, V., Iyer, A., Maeda, H. and Christophi, C. (2009) Styrene maleic acid-pirarubicin disrupts tumor microcirculation and enhances the permeability of colorectal liver metastases. J. Vasc. Res. **46**, 218–228.

85) Suzuki, M., Hori, K., Abe, I., Saito, S. and Sato, H. (1981) A new approach to cancer chemotherapy: selective enhancement of tumor blood flow with angiotensin II. J. Natl. Cancer Inst. **67**, 663–669.

86) Hori, K., Suzuki, M., Tanda, S., Saito, S., Shinozaki, M. and Zhang, Q.H. (1991) Fluctuations in tumor blood flow under normotension and the effect of angiotensin II-induced hypertension. Jpn. J. Cancer Res. **82**, 1309–1316.

87) Li, C.J., Miyamoto, Y., Kojima, Y. and Maeda, H. (1993) Augmentation of tumour delivery of macromolecular drugs with reduced bone marrow delivery by elevating blood pressure. Br. J. Cacner **67**, 975–980.

88) Nagamitsu, A., Greish, K. and Maeda, H. (2009) Elevating blood pressure as a strategy to increase tumor targeted delivery of macromolecular drug SMANCS: cases of advanced solid tumors. Jpn. J. Clin. Oncol. **39**, 756–766.

89) Seki, T., Fang, J. and Maeda, H. (2009) Enhanced delivery of macromolecular antitumor drugs to tumors by nitroglycerin application. Cancer Sci. **100**, 2426–2430.

90) Maeda, H. (2010) Nitroglycerin enhances vascular blood flow and drug delivery in hypoxic tumor tissues: analogy between angina pectoris and solid tumors and enhancement of the EPR effect. J. Control. Release **142**, 296–298.

91) Feelisch, M. and Noack, E. (1987) Correlation between nitric oxide formation during degradation of organic nitrates and activation of guanylate cyclase. Eur. J. Pharmacol. **139**, 19–30.

92) Fukuto, J.M., Cho, J.Y. and Switzer, C.H. (2000) The chemical properties of nitric oxide and related nitrogen oxides. *In* Nitric Oxide: Biology and Pathobiology (ed. Ignarro, L.J.). Academic Press, San Diego, pp. 23–39.

93) Mitchell, J.B., Wink, D.A., DeGraff, W., Gamson, J., Keefer, L.K. and Krishna, M.C. (1993) Hypoxic mammalian cell radiosensitization by nitric oxide. Cancer Res. **53**, 5845–5848.

94) Yasuda, H., Yamaya, M., Nakayama, K., Sasaki, T., Ebihara, S., Kanda, A., Asada, M., Inoue, D., Suzuki, T., Okazaki, T., Takahashi, H., Yoshida, M., Kaneta, T., Ishizawa, K., Yamanda, S., Tomita, N., Yamasaki, M., Kikuchi, A., Kubo, H. and Sasaki, H. (2006) Randomized phase II trial comparing nitroglycerin plus vinorelbine and cisplatin with vinorelbine and cisplatin alone in previously untreated stage IIIB/IV non-small cell lung cancer. J. Clin. Oncol. **24**, 688–694.

95) Yasuda, H., Nakayama, K., Watanabe, M., Suzuki, S., Fuji, H., Okinaga, S., Kanda, A., Zayazu, K., Sasaki, T., Asada, M., Suzuki, T., Yoshida, M., Yamanda, S., Inoue, D., Kaneta, T., Kondo, T., Takai, Y., Sasaki, H., Yanagihara, K. and Yamaya, M. (2006) Nitroglycerin treatment may increase response to docetaxel and carboplatin regimen via inhibitions of hypoxia-inducible factor-1 pathway and P-glycoprotein in patients with lung adenocarcinoma. Clin. Cancer Res. **12**, 6748–6757.

96) Yasuda, H., Yanagihara, K., Nakayama, K., Mio, T., Sasaki, T., Asada, M., Yamaya, M. and Fukushima, M. (2010) Therapeutic applications of nitric oxide for malignant tumor in animal models and human studies. *In* Nitric Oxide and Cancer (ed. Bonavida, B.). Springer Science, New York, pp. 419–441.

97) Siemens, D.R., Heaton, J.P.W., Adams, M.A., Kawakami, J. and Graham, C.H. (2009) Phase II study of nitric oxide donor for men with increasing prostate-specific antigen level after surgery or radiotherapy for prostate cancer.

Urology **74**, 878–883.
98) Jordan, B.F., Misson, P.D., Remeure, R., Baudelet, C., Beghein, N. and Gallez, B. (2000) Changes in tumor oxygenation/perfusion induced by the no donor, isosorbide dinitrate, in comparison with carbogen: monitoring by EPR and MRI. Int. J. Radiat. Oncol. Biol. Phys. **48**, 565–570.
99) Noguchi, A., Takahashi, T., Yamaguchi, T., Kitamura, K., Noguchi, A., Tsurumi, H., Takashina, K. and Maeda, H. (1992) Enhanced tumor localization of monoclonal antibody by treatment with kininase II inhibitor and angiotensin II. Jpn. J. Cancer Res. **83**, 240–243.
100) Hori, K., Saito, S., Takahashi, H., Sato, H., Maeda, H. and Sato, Y. (2000) Tumor-selective blood flow decrease induced by an angiotensin converting enzyme inhibitor, temocapril hydrochloride. Jpn. J. Cancer Res. **91**, 261–269.

(Received Aug. 19, 2011; accepted Jan. 17, 2012)

Profile

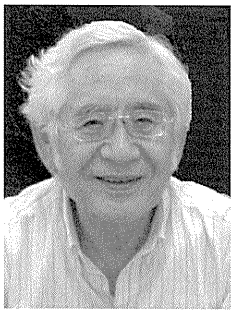

Hiroshi Maeda, born in 1938 and received BS from Tohoku University, started his research carrier since 1964 at Department of Bacteriology, Tohoku University Medical School, Sendai, Japan, after completing MS degree from University of California, Davis, CA as Fulbright student. He studied biochemical characterization of an antitumor protein neocarzinostatin [NCS] isolated from *Streptomyces*, and then completed the amino acid sequence at Children's Hospital/Harvard Medical School, Boston. He was conferred Ph.D., and M.D. degree from Tohoku University. After moving to Kumamoto University Medical School 1971, he studied molecular mechanism of pathogenesis of infection, and discovered two unique pathological events; (i) bradykinin yielding protease cascade (kalikrein-kinin system) and (ii) induction of superoxide generation and nitric oxide synthase, both upon microbial infections.

Another line of research he undertook was on the tumor drug delivery. He pioneered synthesis of the first polymer conjugated antitumor drug (NCS) in 1978, designated SMANCS. SMANCS, being highly lipophilic, it could be solubulized in lipid contrast agent Lipiodol, and developed arterial injection therapy of SMANCS/Lipiodol with Toshimitsu Konno. By this way drug will target to and remain in tumor selectively for several weeks. This therapeutic modality was approved by Japanese Government in 1993. Meantime, he discovered tumor accumulation mechanism of macromolecules. Namely, the drug size larger than 40 KDa exhibited tumor selective accumulation. As a result, ratio of drug in tumor to normal tissues could be more than 20 to 100 in favor of tumor, and they remained in the tumor for weeks. This phenomenon of enhanced permeability and retention effect in solid tumor was coined EPR-effect of macromolecules in 1986. This discovery of EPR-effect paved the way to the tumor drug delivery using nanomedicine. He was professor of Microbiology of Kumamoto University Medical School (1981–2004), then upon retirement moved to Sojo University Faculty of Pharmaceutical Sciences till now. He received many awards such as Award form Princess Takamatsu Cancer Research Fund, Asakawa Award of Japanese Bacteriological Society, Tomizo Yoshida Award from Japan Cancer Association, Gold Medal Award from Frey-Werle Foundation, Germany, Nishinippon Culture Award from Nishinippon Shimbun, Fukuoka, Japan, Nagai Outstanding Innovation Award from Controlled Release Society, U.S.A., among others.

CRS Leading Delivery Science and Technology

Newsletter

A publication of the Controlled Release Society Volume 29 • Number 1 • 2012

What's Inside

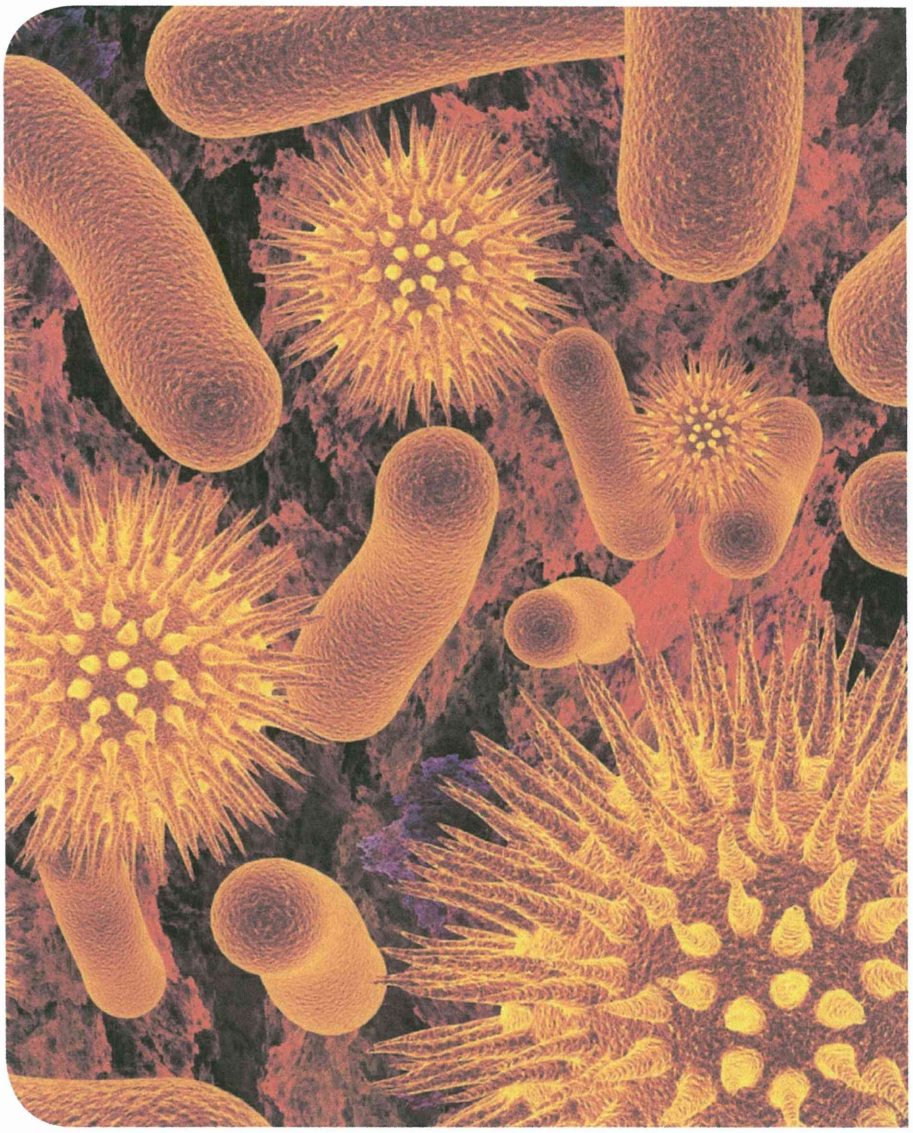

Styrene-co-maleic Acid (SMA) Telomeric Micelles Encapsulated-Zinc Protoporphyrin (SMA-ZnPP) and Other Drugs: Stability Study

Gahininath Y. Bharate,[1,2] Hideaki Nakamura,[1] Jun Fang,[1] Seiji Shinkai,[2] and Hiroshi Maeda[1,2]

A number of natural or synthetic polymers are used as micelle-forming agents. Among them we developed styrene-maleic acid copolymer (SMA) for this purpose. SMA has been used as a car and flour polishing agent and for seizing in the paper industry. Recently, it was approved as a food additive by the U.S. Food and Drug Administration. Use of SMA for pharmaceutical purposes was first started by Maeda's group. Namely, SMA was conjugated with neocarzinostatin (NCS) to make the macromolecular anticancer drug SMANCS.[1,2]

SMA is soluble in organic solvents as well as water. The anhydride group is reactive toward primary amino groups and forms a maleyl amide linkage. In the case of SMANCS, SMA confers high lipophilicity so that SMANCS becomes lymphotropic, a preferred character for the control of lymphatic metastasis. SMA also confers an albumin-binding character.[3,4,5] A lipophilic nature had the advantage of forming an oily formulation in a lipid contrast agent (Lipiodol®).[4] This method led to a new strategy for most tumor-targeting drug delivery using SMANCS/Lipiodol that is administered into the tumor-feeding artery with a catheter, yielding remarkable tumor regression in the most difficult-to-treat cancers, such as primary metastatic liver cancers and renal cancer.[6]

In the past several years, we found that SMA is one of the most versatile micelle-forming agents in that the procedure is simple with reasonable biocompatibility. Another unique aspect of SMA micelles is their stability upon lyophilization and complete recovery of the micelles by adding water, or stability *in vivo*. We found that the micelles only undergo disruption under severe conditions in alkaline or with detergents. More importantly, the drug is released upon internalization into the cells.[7] Recently, SMA micelles of photosensitizers such as Rose Bengal and methylene blue were found to be reasonably stable, to exhibit the enhanced permeability and retention (EPR) effect *in vivo*, and to be applicable for imaging (*unpublished data*).

Experimentals

In this newsletter, we present the stability of SMA micelles containing ZnPP (SMA-ZnPP) and other low-molecular-weight drug candidates. The SMA-ZnPP micelles were prepared very simply by adjusting the pH to >8.0 and then precipitating by acid, followed by dialysis.[8] In this study, two types of SMA, maleylcarboxylated and partially butylated, were used. The nanomicelles thus formed were characterized by UV absorption, fluorescence spectroscopy, Fourier transform infrared spectroscopy (FTIR), dynamic light scattering, zeta potential, and Sephadex G-100 chromatography, as well as biological evaluation.

Stability experiments were based on fluorescence spectroscopy of SMA-ZnPP micelles under different conditions. A release study of ZnPP from SMA micelles was performed by placing the micelle solution (0.5 mg/mL) in dialysis tubes with cut-off molecular mass of 10 kDa against 0.1 M phosphate buffered saline ranging from pH 6.0 to 9.0 at 37°C under stirring.

Results and Discussion

The characterization of two types of SMA-ZnPP micelles is summarized in Table 1.

Free ZnPP in dimethylsulfoxide (DMSO) or in alkaline solution showed the strongest fluorescence in the 580–610 nm range upon excitation at 420.0 nm. However, when SMA-ZnPP was dissolved in aqueous solutions, it was quenched completely, and it appears to exist as a densely stacked form (Figure 1). This suggests that SMA-ZnPP behaves as an encapsulated micellar structure, having π–π interaction of the stacked up state of the tetrapyrrole ring, which suppresses fluorescence due to energy transfer in aqueous solution. Similar phenomena were observed for the micellar drugs using SMA containing doxorubicin and pirarubicin and other fluorescent probes (e.g., Rose Bengal and methylene blue).

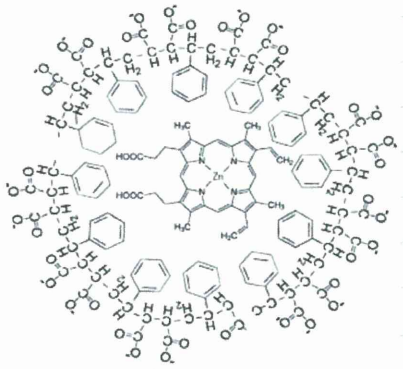

Figure 1. *Schematic representation of SMA-ZnPP micelle.*

Using fluorescence spectroscopy, we investigated the stability of SMA-ZnPP micelles at different pH (6.0–11.0). As shown in Figure 2A and B, weak fluorescence was seen below pH 6.0, which starts to emerge at higher pH, indicating the disintegration of the micelle structure (Figure 2A). A similar phenomenon is seen in the presence of a high concentration of urea and detergent (sodium dodecyl sulfate [SDS]) (Figure 2C

[1] Research Institute for Drug Delivery Systems, Faculty of Pharmaceutical Sciences, Sojo University, Ikeda 4-22-1, Kumamoto, 8600082, Japan.
[2] Department of Nanoscience and Applied Chemistry, Graduate School of Engineering, Sojo University, Ikeda 4-22-1, Kumamoto, 8600082, Japan.

Table 1. Characterization of SMA-ZnPP

SMA Micelle	% Yield (based on ZnPP)	% ZnPP Loading	Mean Particle Size (nm)	Mean Mw by Sephadex G-100	Zeta Potential (ζ, mV)[a]
Carboxy SMA-ZnPP	85	43.5	26.6	115	–46.85
Butyl SMA-ZnPP	92	34.3	29.3	128	–29.13

[a] Zeta potential was determined by Photal model ELSZ (Otsuka Electronics, Osaka, Japan) in 0.1 M phosphate buffer (pH 7.5).

and D), suggesting the disruption of micelle structure by hydrogen bond breakage or by counter ions.

Adequate disintegration of the micelle drugs is an important character, so as to provide the active ingredient access to the molecular target in the cells. SMA micelles were found to undergo disintegration in the presence of lecithin similar to SDS.[7] More importantly, we found SMA-ZnPP micelles were

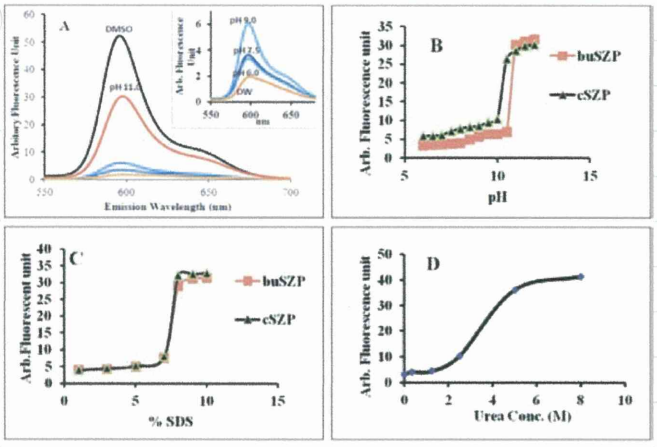

Figure 2. *Fluorescence spectrums of free ZnPP and SMA-ZnPP were recorded on F-4500 spectrofluorometer (Hitachi, Tokyo). (A) The fluorescence spectra of free ZnPP in DMSO and SMA-ZnPP in different pHs; the concentration of ZnPP and SMA-ZnPP was 1 μM (ZnPP equivalent) each. (B) Disintegration of SMA-ZnPP micelles is seen by abrupt increase of fluorescence intensity (at 595 nm) at or above pH 10.5. Stability of the SMA-ZnPP micelles in SDS (C) and Urea (D) is shown.*

disintegrated upon endocytotic uptake, a similar result to exposure to lecithin.[7] This means SMA micelles have ideal drug-release properties, predominantly in the cell after cellular uptake.

The inflection point for butyl SMA-ZnPP micelles was pH 10.5, whereas carboxy SMA-ZnPP was pH 10.0, indicating that butylated SMA was more stable than carboxy SMA. Moreover, Sephadex G-100 chromatography of carboxy SMA-ZnPP showed the apparent molecular size in an aqueous system was about 115 kDa. However, in the presence of albumin, it exhibited 152 kDa, indicating that albumin could bind to SMA-ZnPP micelles.

Zero-order release rate of free ZnPP from its SMA micelles was observed in the pH range of 6.0–9.0 (data not shown). The release rate was found to be a little higher at pH 9.0 (3.0%/day) than at the lower pH 6.0 (2.25%/day).

Conclusion

SMA was found to have a versatile nanomicelle-forming capacity. The micelles can be prepared simply, encapsulating various agents, just by changing pH, consisting of primarily SMA and the drug. All the SMA-drug micelles were proven to be stable during lyophilization and showed a very slow drug-release rate at a wide range of pH. More importantly, it exhibited drug release upon internalization into the cells.[7]

Acknowledgements

This work was supported by Grants-in-Aid, a grant from the Ministry of Health and Welfare (No. 23000001, H23-3) 3rd Cancer Study Project of Japan, and Grants-in-Aid for Scientific Research on Cancer Priority Areas (20015045) and (S0801085) from the MESCT Japan to Hiroshi Maeda. Gahininath Bharate wants to thank BioDynamics Research Foundation, Japan, for a doctoral fellowship.

References

1. Maeda, H, Takeshita, J, Kanamaru, R. A lipophilic derivative of neocarzinostatin, a polymer conjugation of an antitumor protein antibiotic, Int. J. Pept. Protein Res. 14: 81-87 (1979).
2. Maeda, H, Ueda, M, Morinaga, T, Matsumoto, T. Conjugation of poly(styrene-co-maleic acid) derivatives to the antitumor protein neocarzinostatin: Pronounced improvements in pharmacological properties, J. Med. Chem. 28: 455-461 (1985).
3. Takeshita, J, Maeda, H, Kanamaru, R. *In vitro* mode of action, pharmacokinetics, and organ specificity of poly(maleic acid-styrene)-conjugated neocarzinostatin, SMANCS, Gann Jpn. J. Cancer Sci. 73: 278-284 (1982).
4. Oka, K, Miyamoto, Y, Matsumura, Y, Tanaka, S, Oda, T, Suzuki, F, Maeda, H. Enhanced intestinal absorption of a hydrophobic polymer-conjugated protein drug, SMANCS, in an oily formulation, Pharm. Res. 7: 852-855 (1990).
5. Kobayashi, A, Oda, T, Maeda, H. Protein binding of macromolecular anticancer agent SMANCS: Characterization of poly(styrene-co-maleic acid) derivatives as an albumin binding ligand, J. Bioact. Compat. Polym. 3: 319-332 (1988).
6. Nagamitsu, A, Greish, K, Maeda, H. Elevating blood pressure as a strategy to increase tumor-targeted delivery of macromolecular drug SMANCS: Cases of advanced solid tumors, Jpn. J. Clin. Oncol. 39: 756-766 (2009).
7. Nakamura, H, Fang, J, Gahininath, B, Tsukigawa, K, Maeda, H. Intracellular uptake and behavior of two types zinc protoporphyrin (ZnPP) micelles, SMA-ZnPP and PEG-ZnPP as anticancer agents; unique intracellular disintegration of SMA micelles, J. Controlled Release 155: 367-375 (2011).
8. Iyer, AK, Greish, K, Fang, J, Murakami, R, Maeda, H. High-loading nanosized micelles of copoly(styrene-maleic acid)-zinc protoporphyrin for targeted delivery of a potent heme oxygenase inhibitor, Biomaterials 28: 1871-1881 (2007). ■

Cancer Science
The official journal of the Japanese Cancer Association

Carbon monoxide, generated by heme oxygenase-1, mediates the enhanced permeability and retention effect in solid tumors

Jun Fang,[1,5] Haibo Qin,[1,2,5] Hideaki Nakamura,[1] Kenji Tsukigawa,[1,3] Takashi Shin[2] and Hiroshi Maeda[1,3,4]

[1]Laboratory of Microbiology and Oncology, Faculty of Pharmaceutical Sciences, Sojo University, Kumamoto; [2]Department of Applied Microbial Technology, Faculty of Biotechnology and Life Science, Sojo University, Kumamoto; [3]DDS Research Institute, Sojo University, Kumamoto, Japan

(Received August 24, 2011/Revised December 1, 2011/Accepted December 4, 2011/Accepted manuscript online December 6, 2011/Article first published online January 16, 2012)

The enhanced permeability and retention (EPR) effect is a unique pathophysiological phenomenon of solid tumors that sees biocompatible macromolecules (>40 kDa) accumulate selectively in the tumor. Various factors have been implicated in this effect. Herein, we report that heme oxygenase-1 (HO-1; also known as heat shock protein 32) significantly increases vascular permeability and thus macromolecular drug accumulation in tumors. Intradermal injection of recombinant HO-1 in mice, followed by i.v. administration of a macromolecular Evans blue–albumin complex, resulted in dose-dependent extravasation of Evans blue–albumin at the HO-1 injection site. Almost no extravasation was detected when inactivated HO-1 or a carbon monoxide (CO) scavenger was injected instead. Because HO-1 generates CO, these data imply that CO plays a key role in vascular leakage. This is supported by results obtained after intratumoral administration of a CO-releasing agent (tricarbonyldichlororuthenium(II) dimer) in the same experimental setting, specifically dose-dependent increases in vascular permeability plus augmented tumor blood flow. In addition, induction of HO-1 in tumors by the water-soluble macromolecular HO-1 inducer pegylated hemin significantly increased tumor blood flow and Evans blue–albumin accumulation in tumors. These findings suggest that HO-1 and/or CO are important mediators of the EPR effect. Thus, anticancer chemotherapy using macromolecular drugs may be improved by combination with an HO-1 inducer, such as pegylated hemin, via an enhanced EPR effect. (*Cancer Sci* 2012; 103: 535–541)

Conventional chemotherapy with small molecule drugs has been used for many types of cancer for decades. However, the therapeutic efficacy remains less than optimal, mostly because of a lack of tumor selectivity, which results in severe adverse side effects and prevents the use of high drug doses.[1] The development of tumor-targeted chemotherapy is critically important for more successful treatment.

During investigations of targeting drugs to tumors, Matsumura and Maeda[2] found that macromolecular agents larger than 40 kDa selectively accumulate and remain in tumor tissues for long periods. This unique phenomenon in the blood vasculature of solid tumor tissues is quite different from that in normal tissues and was attributed to the unique anatomic and pathophysiologic characteristics of solid tumors. These features include: (i) extensive angiogenesis and hence high vascular density;[3,4] (ii) extensive extravasation (vascular permeability) induced by various vascular mediators, including bradykinin,[5–7] nitric oxide (NO),[7,8] vascular endothelial growth factor (VEGF),[9,10] prostaglandins produced via cyclo-oxygenases,[7] and matrix metalloproteinases;[11] (iii) defective vascular architecture, such as the lack of a smooth muscle layer and large gaps between vascular endothelial cells;[12,13] and (iv) impaired lymphatic clearance from the tumor interstitial space.[14–16] The increased vascular permeability and defective vascular structure allow molecules larger than those subject to renal clearance (i.e. ≥40 kDa) to extravasate gradually, over a long time, into the interstitial space in tumor tissues. Furthermore, the molecules remain in the interstitial space without being cleared because of the impaired lymphatic system in tumors.[2,13–16] This phenomenon was named the enhanced permeability and retention effect (EPR effect) in solid tumors.

In previous studies, we have shown that this EPR effect can be augmented and drug delivery improved two- to threefold[16–20]. One approach used angiotensin (Ang) II-induced hypertension, during which tumor blood flow was increased selectively.[16,17] The AngII-induced augmentation of the EPR effect was validated not only in animal experiments, but also in the clinical setting with difficult-to-treat tumors.[18,19] Another approach involved using NO-generating agents such as nitroglycerin (NTG), which significantly increased the accumulation of macromolecular drugs in tumors.[20]

In a completely different series of experiments, we have been working on heme oxygenase-1 (HO-1), known as a key factor for supporting rapid tumor growth, as an anticancer target.[21–24] Heme oxygenase is a key enzyme in heme metabolism, with products including biliverdin, carbon monoxide (CO), and free iron (Fe^{3+}); biliverdin is subsequently converted to bilirubin.[25,26] Numerous studies have demonstrated important physiological roles of CO, comparable to those of NO, including vascular dilatation, facilitation of vascular blood flow, and antioxidative and antiapoptotic effects.[27–29] We thus hypothesized that CO-generating HO-1 may serve as another factor mediating the EPR effect and may be useful in augmenting chemotherapeutic effects.

In the present study, we used recombinant HO-1 and a CO-releasing agent to investigate the effects of HO-1 and CO on vascular permeability. In addition, by using the water-soluble macromolecular HO-1 inducer pegylated hemin (PEG-hemin), we verified the CO- and HO-1-induced augmentation of the EPR effect in a murine solid tumor model.

Materials and Methods

Materials. Tricarbonyldichlororuthenium(II) dimer (CORM-2), zinc protoporphyrin-IX (ZnPP), and hemin were purchased from Sigma-Aldrich Chemical (St Louis, MO, USA). Other chemicals of reagent grade were from Wako Pure Chemical Industries (Osaka, Japan) and were used without further purification.

Animals. Male ddY mice, 6 weeks old and weighing 30–35 g, and male SD rat weighing 200-250 g were obtained from Kyudo (Kumamoto, Japan). Mice were maintained under

[4]To whom correspondence should be addressed.
E-mail: hirmaeda@ph.sojo-u.ac.jp
[5]These authors contributed equally to this work.

doi: 10.1111/j.1349-7006.2011.02178.x

standard conditions (12-h dark–light cycle, 23 ± 1°C). All experiments were performed according to the guidelines of the Laboratory Protocol of Animal Handling, Sojo University.

Preparation of recombinant HO-1 protein. Total mRNA was extracted from rat liver using the Takara RNA PCR Kit (AMV) Ver. 3.0 (Takara Bio, Otsu, Japan), with HO-1 cDNA being amplified with HO-1 Cf (gatcagcactagttcatcccagacataacctag) and HO-1 Cr (gttatgtctgggatgaactagtgct) primers using KOD FX polymerase (Takara). Rat HO-1 cDNA was then inserted into the pET3c vector through the *Nde*1 and *Bam*H1 restriction enzyme sites located at the 5′ and 3′ ends, respectively.

Escherichia coli Rosetta-gami (DE3) bacteria harboring the abovementioned pET3c plasmid encoding rat HO-1 were cultured in LB medium containing 50 μg/mL ampicillin and 20 μg/mL chloramphenicol. The HO-1 protein was induced by addition of 10 μM isopropyl β-D-thiogalactopyranoside. After 6 h incubation at 37°C with shaking, the bacterial pellet was sonicated (150 W, 20 min) in 50 mM Tris–HCl buffer (pH 8.0) with protease inhibitors (2 mM phenylmethylsulfonyl fluoride and 10 μg/mL leupeptin) at 4°C. Then, rat HO-1 was partially purified by using ammonium sulfate precipitation (30–60% fraction), after which it was dialyzed against 10 mM potassium phosphate buffer (pH 7.4). It was finally purified by using a DEAE negative ion exchange column; 10 mM phosphate buffer (pH 7.4) containing 250 mM KCl was used for gradient elution. The purity of the rat HO-1 was demonstrated to be >90% using SDS-PAGE with Coomassie brilliant blue staining.

Synthesis of PEG-hemin. The synthesis, purification, and characterization of PEG-hemin were as described previously.[30]

Determination of the effect of HO-1, HO-1 inhibitors, and CO on vascular permeability in normal mouse skin. The ddY mice were anesthetized with sodium pentobarbital (83 mg/kg, i.p.). Test samples (50 μL each) were injected intradermally (i.d.) into the dorsal skin of mice, followed immediately by i.v. injection of 10 mg/kg Evans blue dye. Mice were killed 2 h after injection of Evans blue and the amount of extravasated dye in the skin at the site of injection was quantified after extraction with formamide, as described previously.[2] Similar experiments were performed with an *in vivo* imaging system (NightOWL II; Berthold Technologies, Bad Wildbad, Germany) using a macromolecular fluorescent dye (i.e. rhodamine-conjugated bovine albumin synthesized in our laboratory; Hideaki Nakamura, Jun Fang, Haibo Qin, Gahininath Y Bharate, Hiroshi Maeda, unpublished data, 2011) instead of Evans blue, with excitation and emission at 540 and 600 nm, respectively.

Induction of HO-1 activity by PEG-hemin in sarcoma 180 tumors in mice. Mouse sarcoma S180 cells (2×10^6) were injected s.c. into the dorsal skin of ddY mice. Approximately 8–10 days later, when tumor diameters measured 7–10 mm, PEG-hemin (10 mg/kg hemin equivalent), which is a water-soluble macromolecular HO-1 inducer, was injected i.v. After 24 h, mice were killed; both tumors and normal tissues (liver, muscle) were removed and weighed, with microsomal fractions of each tissue obtained by ultracentrifugation to be used for measurement of HO-1 activity, as described previously.[24,31]

Quantification of CO in S180 tumor-bearing mice after PEG-hemin treatment. The PEG-hemin was administered to ddY mice bearing S180 solid tumors as described above. Twenty-four hours later, mice were killed and blood was collected, with a 0.35-mL aliquot of the blood sample diluted with 3.65 mL of 0.01 M PBS (pH 7.2) and placed in a 10-mL glass test tube on ice. The blood was then purged with nitrogen gas, after which the NO donor 3-(2-hydroxy-1-methyl-2-nitrosohydrazino)-*N*-methyl-1-propanamine (NOC-7; Dojin Chemical, Kumamoto, Japan) was added to a final concentration of 1 mM. The test tube was then sealed using paraffin. Under these conditions, excessive NO generated would bind to hemoglobin, so CO would be released instead. After 2 h incubation at room temperature, 1 mL of the gas in the test tubes was used for CO quantification by gas chromatography (TRIlyzer mBA-3000; TAIYO Instruments, Osaka, Japan).

Effect of HO-1 on tumor vascular permeability (EPR effect) in S180 tumor-bearing mice. To induce HO-1 in tumors, S180 tumor-bearing ddY mice were injected with 10 mg/kg, i.v., PEG-hemin. After 24 h, 10 mg/kg, i.v., Evans blue was injected. Then, 24 h after injection of Evans blue, the mice were killed, both the tumors and normal tissues (liver, spleen, and kidney) were removed, and the amount of extravasated dye in the tumors and normal tissues was quantified as described previously.[2]

Measurement of tumor blood flow. A laser Doppler flowmeter (ALF21; Advance, Tokyo, Japan) was used to measure blood flow in tumors and normal tissues (liver and muscle) in 10 mg/kg PEG-hemin-treated and control mice. In each mouse, the flowmeter probe was inserted into non-necrotic tumor tissues and blood flow was monitored for 5–10 min until it stabilized.

The effect of CO on tumor blood flow was investigated using the same method, with the exception that mice received intratumoral (i.t.) injections of CORM-2 (25 nmol in 0.05 mL), and real-time changes in tumor blood flow before and after CORM-2 administration were monitored. Measurements were obtained in anesthetized (sodium pentobarbital) mice, as described above.

Statistical analysis. All data are expressed as the mean ± SEM. The significance of differences was evaluated using Student's *t*-test, with significance set at $P < 0.05$.

Results

Enhanced vascular permeability in normal mouse skin following HO-1 injection. It was evident that HO-1 induced dose-dependent increases in vascular permeability in normal dorsal mouse skin (Fig. 1). However, injection of heat-inactivated (100°C, 5 min) HO-1 had a significantly reduced effect (Figs 1,2), which suggests that the enzymatic activity of HO-1 is necessary for it to enhance vascular permeability. Moreover, the extravasation induced by HO-1 decreased significantly when HO-1 was mixed with BSA, a major bilirubin-binding and probably CO-binding protein in plasma (Fig. 1). The HO-1 inhibitor ZnPP completed abolished this effect of HO-1 on vascular permeability, as assessed using an *in vivo* imaging system, as described below (Fig. 2). In addition, ZnPP did not significantly decrease the vascular permeability triggered by NO (see Fig. S1), which is considered to occur via the activation of soluble guanylate cyclase (sGC), suggesting the effect of ZnPP on HO-1 induced vascular permeability, at the concentrations used in the present study, is due mostly to inhibition of HO-1, although ZnPP has also been reported to inhibit sGC independent of HO-1.[32]

More importantly, administration of the CO scavenger hemoglobin completely abolished the enhanced vascular permeability produced by HO-1 (Fig. 2). These data suggest that CO has an essential role in HO-1-induced vascular permeability.

Effect of CO on vascular permeability. To validate the role of CO in vascular permeability, the CO-releasing agent CORM-2 was used in the same vascular permeability study. As shown in Figure 3, CORM-2, at picomolar levels, had significant, dose-dependent effects on vascular permeability. No such effect was observed when CORM-2 was decomposed by incubation at room temperature for 24 h to completely liberate CO (Fig. 3). Moreover, ZnPP had no effect on the CORM-2-derived CO-induced increase in vascular permeability (Fig. S1).

Induction of HO-1 in tumor tissue by PEG-hemin. We developed PEG-hemin, a water-soluble pegylated HO-1 inducer, in our laboratory.[30] It behaves as a macromolecular micelle with a molecular mass of 126 kDa, and so may accumulate selectively in solid tumors based on the EPR effect. Accordingly, to

doi: 10.1111/j.1349-7006.2011.02178.x

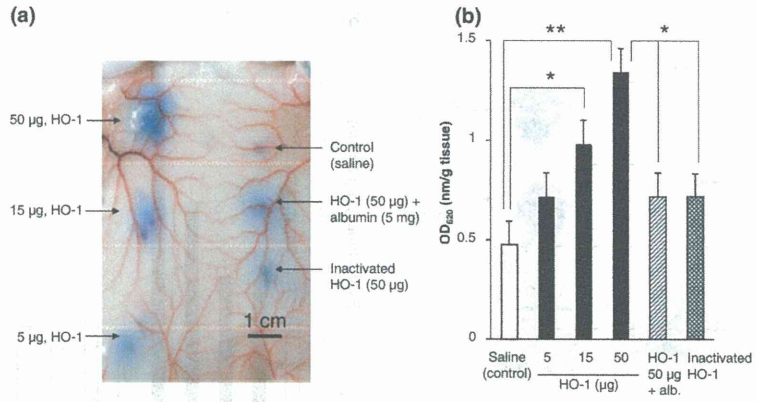

Fig. 1. Effect of heme oxygenase-1 (HO-1) on vascular permeability of the dorsal skin in normal mice. Recombinant HO-1 protein and other agents were administered i.d., followed by i.v. injection of Evans blue (10 mg/kg). The dye was allowed to extravasate for 2 h. (a) Representative image showing the extravasation of blue dye caused by each agent. (b) Quantification of the extravasation of Evans blue from the skin tissues. Alb, albumin. Data are the mean ± SEM (n = 3–4). *P < 0.05, **P < 0.01.

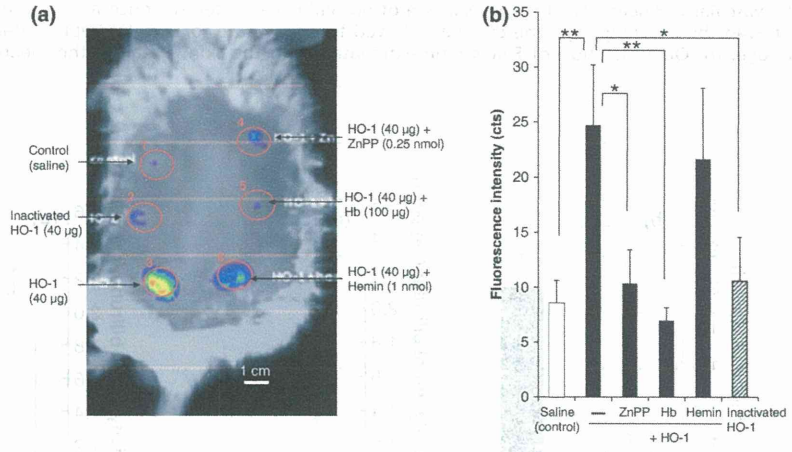

Fig. 2. Vascular permeability induced by heme oxygenase-1 (HO-1) and its inhibition in normal mice, as evaluated using an *in vivo* imaging system. The HO-1 protein, with or without its inhibitor zinc protoporphyrin-IX (ZnPP) or the carbon monoxide scavenger hemoglobin (Hb), was administered i.d., followed by i.v. injection of the macromolecular fluorescent dye rhodamine-conjugated bovine albumin (5 mg/kg rhodamine equivalent). The dye was allowed to extravasate for 1 h. (a) Representative image showing authentic HO-1-induced vascular permeability. (b) Quantification of data. Data are the mean ± SEM (n = 3–4). *P < 0.05, **P < 0.01.

investigate the role of HO-1 in the permeability of the tumor vasculature, we used PEG-hemin to induce HO-1 in S180 solid tumors. As expected, HO-1 activity in tumor tissues was increased significantly after PEG-hemin treatment (Fig. 4a).

We further confirmed this finding by measuring CO concentrations in the circulation, because we have found that circulating levels of CO are positively related to tumor growth and HO-1 activity in tumors (Jun Fang, Takaaki Akaike, Chiho Taruki, Tomohiro Sawa, Hiroshi Maeda, unpublished observation, 2004). As expected, circulating levels of CO increased significantly after PEG-hemin treatment, which paralleled the increase in HO-1 activity (Fig. 4b).

Moreover, increases in HO activity were not found in normal tissue (e.g. muscle) following injection of PEG-hemin (Fig. 4c). It is known that many macromolecules accumulate in high levels in the liver, primarily through the reticuloendothelial system, and pegylation is widely used to avoid the capturing of macromolecules by the reticuloendothelial clearance system.[33] Thus, in the present study we measured the body distribution of PEG-hemin in S180 tumor-bearing mice; high accumulation of PEG-hemin was observed in tumors and the liver (Fig. S2). However, only non-significant increases in HO activity were observed in the liver after PEG-hemin administration (Fig. 4d). This may be probably due to the endogenous presence of a high HO content in the liver and spleen, which are the major organs for heme catabolism.

Involvement of HO-1 in enhanced vascular permeability in S180 solid tumors. As shown in Figure 5, pretreatment with PEG-hemin, injected i.v., produced significantly greater extravasation of the Evans blue–albumin complex in tumor tissue, but not in normal tissues. This provides clear evidence that the EPR effect was enhanced in the tumor tissue by PEG-hemin.

Effect of HO-1 and CO on tumor blood flow. We hypothesized that HO-1, in addition to augmenting tumor vascular permeability (the EPR effect) as described above, may also improve tumor blood flow, because CO has a vasodilator effect similar to that of NO.[27] Thus, we measured blood flow in S180 solid tumors with and without HO-1 induction by PEG-hemin. As anticipated, tumor blood flow increased significantly, by four- to fivefold, 24 h after i.v. injection of PEG-hemin compared with untreated controls (Fig. 6a). This treatment had no effect on the blood flow of normal tissues

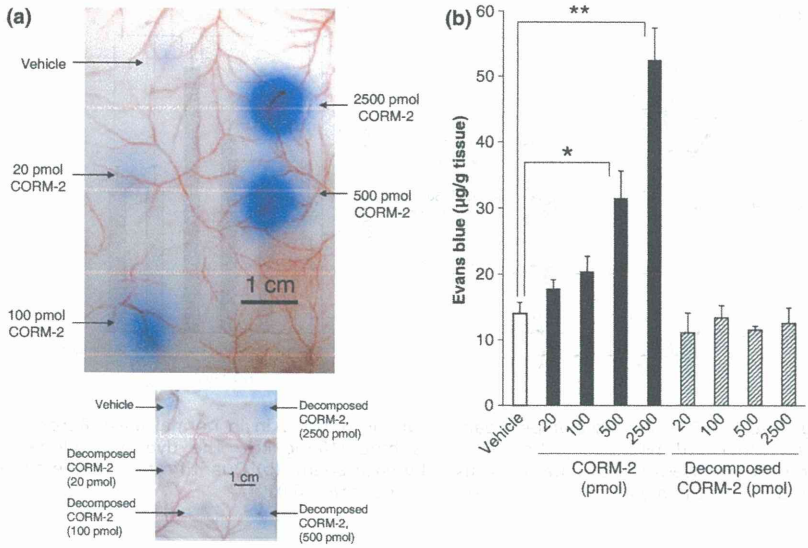

Fig. 3. Effect of CORM-2 on the vascular permeability of the dorsal skin of normal mice. Different concentrations of CORM-2 were administered i.d., followed by i.v. injection of Evans blue (10 mg/kg). The dye was allowed to extravasate for 2 h. (a) Representative images showing CORM-2-induced extravasation of blue dye. (b) Quantification of Evans blue extravasation in the skin. Data are the mean ± SEM (n = 3–4). *P < 0.05, **P < 0.01.

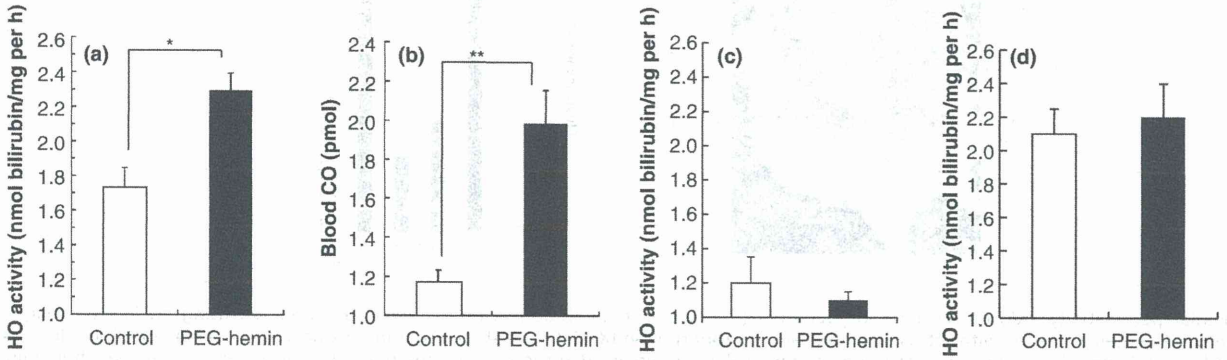

Fig. 4. *In vivo* induction of heme oxygenase-1 (HO-1) in tumors and normal tissues (liver, muscle) after pegylated hemin (PEG-hemin) treatment of tumor-bearing mice. (a) Twenty-four hours after i.v. injection of PEG-hemin (10 mg/kg hemin equivalent), HO-1 activity, as evidenced by bilirubin formation, was determined in the tumors. (b) The induction of HO-1 was verified by measuring blood concentrations of carbon monoxide (CO). (c,d) The HO-1 activity in the liver (c) and muscle (d) was also determined. Data are the mean ± SEM (n = 4). *P < 0.05, **P < 0.01.

(i.e. liver and muscle; data not shown). Furthermore, when CORM-2 was injected directly into tumors, tumor blood flow increased gradually for approximately 2 h, at which time it had increased 1.5–2-fold of levels seen before CORM-2 injection (Fig. 6b).

Discussion

Targeted drug delivery is the key for successful anticancer treatment. In contrast, the use of conventional anticancer drugs results in severe adverse side effects, which prevents the use of higher doses. Consequently, the therapeutic effects of conventional low molecular weight anticancer drugs are limited.

Because of these problems, so-called molecular target therapy has recently come into focus. This type of therapy is designed to target specific receptors or kinases associated with tumor growth, progression, invasion, and metastasis. However, one problem with molecular target therapy is related to the genetic diversity of human solid tumors, in which target molecules may have mutated.[34,35] Another possible problem is that multiple genes may be involved in sophisticated networks that have multiple backup systems for the molecular pathways that are vital for tumor cells. Thus, molecular target therapy, although highly specific for targets, seems to be an approach that would not be able to destroy most, or all, tumor cells.

The discovery of the EPR effect was a considerable breakthrough, leading to a more universal tumor-targeting mechanism at the tissue or vascular level. That is, EPR effect-based targeting depends on the unique anatomic and pathophysiologic features of tumor vessels, which are common to most solid tumors. Thus, EPR effect-based tumor targeting has wider applicability and it is now becoming an increasingly promising paradigm for anticancer drug development.[16,36,37]

We have been seeking to augment the EPR effect even more by using specific features involved in the effect. One example of

doi: 10.1111/j.1349-7006.2011.02178.x

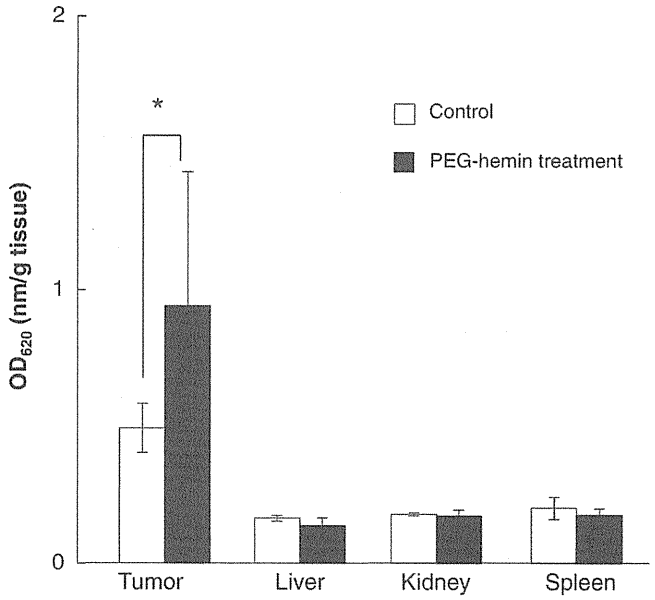

Fig. 5. Accumulation of Evans blue–albumin complex in tumors and normal tissues (liver, kidney, and spleen) after pegylated hemin (PEG-hemin) treatment of tumor-bearing mice. Twenty-four hours after i.v. injection of PEG-hemin (10 mg/kg hemin equivalent), 10 mg/kg, i.v., Evans blue was injected. After a further 24 h, mice were killed and tissues collected. Control mice were not treated with PEG-hemin. The blue dye in each tissue was extracted and the amount was quantified. Data are the mean ± SEM (n = 4). *P < 0.05.

our success was the application of AngII-induced hypertension, which induced a two- to threefold augmentation of the EPR effect without having any effect on the distribution of drug in normal tissues.[16,18,19,38] Another new approach was recently developed with the NO-releasing agent NTG.[20] In hypoxic tumor tissue, NTG is selectively converted to nitrite (NO_2^-), which is then converted to NO in the tumor. This event is analogous to the hypoxic conditions in angina pectoris.[39] Nitric oxide generated from NTG then increases the delivery of macromolecular drugs to the tumor by two- to threefold, resulting in an improved anticancer effect.[20]

In addition, CO has been reported as an important endogenous signaling molecule with various biological functions that include regulation of vascular tonus, being involved in antiapoptosis, having anti-inflammatory effects, and inducing angiogenesis.[27,40] Regarding the effect of CO on vasoregulation, most data support a prodilatory role for CO; however, vasoconstrictor effects of CO have also been reported via inhibition of NO synthesis to antagonize NO-dependent vasodilation[41] or via the induction of a more oxidative stage of the vasculature by CO.[42] These results suggest the complexity of CO-induced vasoregulation: CO is not necessarily a vasorelaxant and may exhibit an opposite effect depending on the milieu. Notwithstanding, we clearly found that CO increased vascular permeability and blood flow in the present study, suggesting a vasodilatory role for CO in the experimental setting in the present study.

The major source (i.e. >80%) of CO in biological systems is HO-catalysed heme degradation.[27] In the present study, we found that HO-1 induced an increase in tumor blood flow (Fig. 6a), which was probably the consequence of the vasorelaxant effect of significantly increased CO levels from HO-1 induced by PEG-hemin. This is supported by the finding that direct injection of CORM-2 into tumors significantly increased tumor blood flow (Fig. 6b). In addition, although circulating levels of CO increased after PEG-hemin treatment, accompanying the increase in HO activity (CO production) in tumors (Fig. 4b), there was no change in vascular permeability (Fig. 5) and blood flow (data not shown) in normal tissues and organs. This is probably because of the capture of CO by hemoglobin and the autoregulatory function (homeostasis) of normal blood vessels to maintain blood volume.

Furthermore, CO was recently reported to induce VEGF expression via p38 kinase-dependent activation of specificity protein 1 (SP1) transcriptional factor,[43] which thus induces angiogenesis. It is known that VEGF is an important vascular permeability factor,[9,10,44,45] probably via activation of

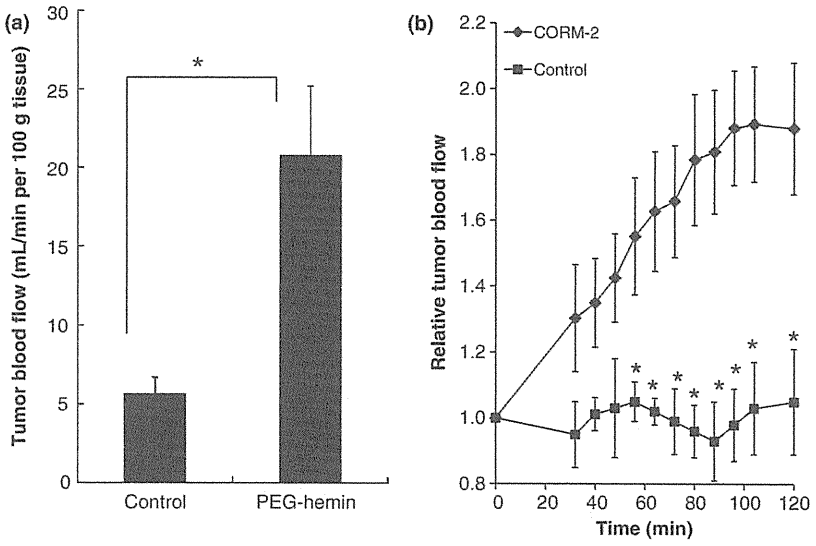

Fig. 6. Changes in tumor blood flow after (a) pegylated hemin (PEG-hemin) and (b) CORM-2 treatment of tumor-bearing mice (control mice were untreated). Mice were injected with either PEG-hemin (10 mg/kg, i.v.) or the indicated concentrations of CORM-2 (intratumoral) and tumor blood flow was measured using a laser Doppler flowmeter. Data are the mean ± SEM (n = 4). *P < 0.05.

endothelial NO synthase to generate NO.[9] We thus believe that VEGF may also be involved in the enhanced vascular permeability induced by HO-1 and CO.

Regarding the vascular pathophysiology of tumors, it should be noted that the role of HO-1 is not always same as that of CO and will vary depending on the cell context and tumor microenvironment.[46,47] For example, although many studies have reported a proangiogenetic effect of HO-1,[21,48,49] Ferrando *et al.*[47] described an inhibitory effect of HO-1 on angiogenesis in prostate cancer. The mechanism underlying the proangiogenic effect of HO-1 under pathological conditions is not clear and, in tumors, may depend on the type of tumor or other undefined factors. However, in the present study we focused our efforts on clarifying the role of the HO-1 product (CO) in increasing tumor vascular permeability, and not on the effect of HO-1 *per se* on angiogenesis, which involves many pathophysiologic effectors.

In the present study, PEG-hemin induced the expression of HO-1 in tumor cells by accumulating in tumor tissues, which subsequently induced the generation of CO, resulting in increased tumor vascular permeability and blood flow (Fig. 5). On the basis of these findings, we should be able to improve drug delivery to tumors.

In conclusion, in the present study we found that CO is an important mediator of the EPR effect. The CO-releasing agent CORM-2 alone and selective induction of HO-1 expression in tumor by PEG-hemin administered i.v. both significantly improved tumor blood flow and extravasation of macromolecules into the tumor by enhancing the EPR effect. Thus, drug delivery based on the EPR effect was augmented. Because of HO induction, and hence CO generation, PEG-hemin used in combination with chemotherapeutic drugs (especially macromolecular drugs) may hold promise as a new anticancer therapy and warrants further investigation.

Acknowledgments

The authors thank Judith B. Gandy for English language editing of the original manuscript. This work was supported, in part, by Grants-in-Aid from the Ministry of Education, Science, Culture, Sports and Technology of Japan (22700927, 17016076, and 20015405) and a Grant-in-Aid from the Ministry of Welfare, Health and Labor of Japan (H23-sanjig-ann-ippan-001).

Disclosure Statement

The authors declare they have no potential conflicts of interest.

References

1 Hassett MJ, O'Malley AJ, Pakes JR, Newhouse JP, Earle CC. Frequency and cost of chemotherapy-related serious adverse effects in a population sample of women with breast cancer. *J Natl Cancer Inst* 2006; **98**: 1108–17.
2 Matsumura Y, Maeda H. A new concept for macromolecular therapeutics in cancer chemotherapy: mechanism of tumoritropic accumulation of proteins and the antitumor agent SMANCS. *Cancer Res* 1986; **46**: 6387–92.
3 Folkman J. Tumor angiogenesis: therapeutic implications. *N Engl J Med* 1971; **285**: 1182–6.
4 Folkman J, Shing Y. Angiogenesis. *J Biol Chem* 1992; **267**: 10931–4.
5 Maeda H, Matsumura Y, Kato H. Purification and identification of [hydroxyprolyl^3]bradykinin in ascitic fluid from a patient with gastric cancer. *J Biol Chem* 1988; **263**: 16051–4.
6 Matsumura Y, Kimura M, Yamamoto T, Maeda H. Involvement of the kinin-generating cascade in enhanced vascular permeability in tumor tissue. *Jpn J Cancer Res* 1988; **79**: 1327–34.
7 Wu J, Akaike T, Maeda H. Modulation of enhanced vascular permeability in tumors by a bradykinin antagonist, a cyclooxygenase inhibitor, and a nitric oxide scavenger. *Cancer Res* 1998; **58**: 159–65.
8 Maeda H, Noguchi Y, Sato K, Akaike T. Enhanced vascular permeability in solid tumor is mediated by nitric oxide and inhibited by both new nitric oxide scavenger and nitric oxide synthase inhibitor. *Jpn J Cancer Res* 1994; **85**: 331–4.
9 Maeda H, Fang J, Inutsuka T, Kitamoto Y. Vascular permeability enhancement in solid tumor: various factors, mechanisms involved and its implications. *Int Immunopharmacol* 2003; **3**: 319–28.
10 Senger DR, Galli SJ, Dvorak AM, Perruzzi CA, Harvey VS, Dvorak HF. Tumor cells secrete a vascular permeability factor that promotes accumulation of ascites fluid. *Science* 1983; **219**: 983–5.
11 Wu J, Akaike T, Hayashida K, Okamoto T, Okuyama A, Maeda H. Enhanced vascular permeability in solid tumor involving peroxynitrite and matrix metalloproteinases. *Jpn J Cancer Res* 2001; **92**: 439–51.
12 Suzuki M, Takahashi T, Sato T. Medial regression and its functional significance in tumor-supplying host arteries. A morphometric study of hepatic arteries in human livers with hepatocellular carcinoma. *Cancer* 1987; **59**: 444–50.
13 Skinner SA, Tutton PJ, O'Brien PE. Microvascular architecture of experimental colon tumors in the rat. *Cancer Res* 1990; **50**: 2411–7.
14 Iwai K, Maeda H, Konno T. Use of oily contrast medium for selective drug targeting to tumor: enhanced therapeutic effect and X-ray image. *Cancer Res* 1984; **44**: 2115–21.
15 Maeda H, Sawa T, Konno T. Mechanism of tumor-targeted delivery of macromolecular drugs, including the EPR effect in solid tumor and clinical overview of the prototype polymeric drug SMANCS. *J Control Release* 2001; **74**: 47–61.
16 Fang J, Nakamura H, Maeda H. The EPR effect: unique features of tumor blood vessels for drug delivery, factors involved, and limitations and augmentation of the effect. *Adv Drug Deliv Rev* 2010; **63**: 136–51.
17 Suzuki M, Hori K, Abe Z, Asito S, Sato H. A new approach to cancer chemotherapy: selective enhancement of tumor blood flow with angiotensin II. *J Natl Cancer Inst* 1981; **67**: 663–9.
18 Li CJ, Miyamoto Y, Kojima Y, Maeda H. Augmentation of tumor delivery of macromolecular drugs with reduced bone marrow delivery by elevating blood pressure. *Br J Cancer* 1993; **67**: 975–80.
19 Nagamitsu A, Greish K, Maeda H. Elevating blood pressure as a strategy to increase tumor-targeted delivery of macromolecular drug SMANCS: cases of advanced solid tumors. *Jpn J Clin Oncol* 2009; **39**: 756–66.
20 Seki T, Fang J, Maeda H. Enhanced delivery of macromolecular antitumor drugs to tumors by nitroglycerin application. *Cancer Sci* 2009; **100**: 2426–30.
21 Fang J, Akaike T, Maeda H. Antiapoptotic role of heme oxygenase (HO) and the potential of HO as a target in anticancer treatment. *Apoptosis* 2004; **9**: 27–35.
22 Doi K, Akaike T, Fujii S *et al.* Induction of haem oxygenase-1 by nitric oxide and ischaemia in experimental solid tumours and implications for tumour growth. *Br J Cancer* 1999; **80**: 1945–54.
23 Fang J, Sawa T, Akaike T *et al. In vivo* antitumor activity of pegylated zinc protoporphyrin: targeted inhibition of heme oxygenase in solid tumor. *Cancer Res* 2003; **63**: 3567–74.
24 Tanaka S, Akaike T, Fang J *et al.* Antiapoptotic effect of haem oxygenase-1 induced by nitric oxide in experimental solid tumour. *Br J Cancer* 2003; **88**: 902–9.
25 Schacter BA. Heme catabolism by heme oxygenase: physiology, regulation, and mechanism of action. *Semin Hematol* 1988; **25**: 349–69.
26 Maines MD. Heme oxygenase: function, multiplicity, regulatory mechanisms, and clinical applications. *FASEB J* 1988; **2**: 2557–68.
27 Abraham NG, Kappas A. Pharmacological and clinical aspects of heme oxygenase. *Pharmacol Rev* 2008; **60**: 79–127.
28 Nakao A, Kaczorowski DJ, Wang Y *et al.* Amelioration of rat cardiac cold ischemia/reperfusion injury with inhaled hydrogen or carbon monoxide, or both. *J Heart Lung Transplant* 2010; **29**: 544–53.
29 Nakao A, Choi AM, Murase N. Protective effect of carbon monoxide in transplantation. *J Cell Mol Med* 2006; **10**: 650–71.
30 Fang J, Qin H, Seki T *et al.* Therapeutic potential of pegylated hemin for ROS-related diseases via induction of heme oxygenase-1: results from a rat hepatic ischemia/reperfusion injury model. *J Pharmacol Exp Ther* 2011; **339**: 779–89.
31 Drummond GS, Kappas A. Prevention of neonatal hyperbilirubinemia by tin protoporphyrin IX, a potent competitive inhibitor of heme oxygenase. *Proc Natl Acad Sci USA* 1981; **78**: 6466–70.
32 Serfass L, Burstyn JN. Effect of heme oxygenase inhibitors on soluble guanylyl cyclase activity. *Arch Biochem Biophys* 1998; **359**: 8–16.
33 Soloman R, Gabizon AA. Clinical pharmacology of liposomal anthracyclines: focus on pegylated liposomal doxorubicin. *Clin Lymphoma Myeloma* 2008; **8**: 21–32.
34 Wood LD, Parsons DW, Jones S *et al.* The genomic landscapes of human breast and colorectal cancers. *Science* 2007; **318**: 1108–13.

doi: 10.1111/j.1349-7006.2011.02178.x

35 Sjöblom T, Jones S, Wood LD *et al.* The consensus coding sequences of human breast and colorectal cancers. *Science* 2006; **314**: 268–74.
36 Vicent MJ, Ringsdorf H, Duncan R. Polymer therapeutics: clinical applications and challenges for development. *Adv Drug Deliv Rev* 2009; **61**: 1117–20.
37 Matsumura Y, Kataoka K. Preclinical and clinical studies of anticancer agent-incorporating polymer micelles. *Cancer Sci* 2009; **100**: 572–9.
38 Maeda H. Tumor-selective delivery of macromolecular drugs via the EPR effect: background and future prospects. *Bioconjug Chem* 2010; **21**: 797–802.
39 Maeda H. Nitroglycerin enhances vascular blood flow and drug delivery in hypoxic tumor tissues: analogy between angina pectoris and solid tumors and enhancement of the EPR effect. *J Control Release* 2010; **142**: 296–8.
40 Otterbein LE, Bach FH, Alam J *et al.* Carbon monoxide has anti-inflammatory effects involving the mitogen-activated protein kinase pathway. *Nat Med* 2000; **6**: 422–8.
41 Lin HH, Lai SC, Chau LY. Heme oxygenase-1/carbon monoxide induces vascular endothelial growth factor expression via p38 kinase-dependent activation of Sp1. *J Biol Chem* 2011; **286**: 3829–38.
42 Ferrara N, Henzel WJ. Pituitary follicular cells secrete a novel heparin-binding growth factor specific for vascular endothelial cells. *Biochem Biophys Res Commun* 1989; **161**: 851–8.
43 Johnson FK, Johnson RA. Carbon monoxide promotes endothelium dependent constriction of isolated gracilis muscle arterioles. *Am J Physiol Regul Integr Comp Physiol* 2003; **285**: R536–41.
44 Lamon BD, Zhang FF, Puri N, Brodsky SV, Goligorsky MS, Nasjletti A. Dual pathways of carbon monoxide-mediated vasoregulation: modulation by redox mechanisms. *Circ Res* 2009; **105**: 775–83.
45 Keck PJ, Hauser SD, Krivi G *et al.* Vascular permeability factor, an endothelial cell mitogen related to PDGF. *Science* 1989; **246**: 1309–12.
46 Dulak J, Deshane J, Jozkowicz A, Agarwal A. Heme oxygenase-1 and carbon monoxide in vascular pathobiology: focus on angiogenesis. *Circulation* 2008; **117**: 231–41.
47 Ferrando M, Gueron G, Elguero B *et al.* Heme oxygenase 1 (HO-1) challenges the angiogenic switch in prostate cancer. *Angiogenesis* 2011; **14**: 467–79.
48 Sunamura M, Duda DG, Ghattas MH *et al.* Heme oxygenase-1 accelerates tumor angiogenesis of human pancreatic cancer. *Angiogenesis* 2003; **6**: 15–24.
49 Miyake M, Fujimoto K, Anai S *et al.* Heme oxygenase-1 promotes angiogenesis in urothelial carcinoma of the urinary bladder. *Oncol Rep* 2011; **25**: 653–60.

Supporting Information

Additional Supporting Information may be found in the online version of this article:

Fig. S1. Effect of zinc protoporphyrin-IX (ZnPP) on nitric oxide (NO)- or carbon monoxide (CO)-induced vascular permeability.

Fig. S2. Body distribution of pegylated hemin (PEG-hemin) in S180 tumor-bearing ddY mice after i.v. injection.

Please note: Wiley-Blackwell are not responsible for the content or functionality of any supporting materials supplied by the authors. Any queries (other than missing material) should be directed to the corresponding author for the article.

EBM-1110-RM-360

Original Research

Pegylated D-amino acid oxidase restores bactericidal activity of neutrophils in chronic granulomatous disease via hypochlorite

Hideaki Nakamura[1,2], Jun Fang[1,2], Tomoyuki Mizukami[3], Hiroyuki Nunoi[4] and Hiroshi Maeda[2]

[1]Laboratory of Microbiology and Oncology, Faculty of Pharmaceutical Science; [2]Institute for Drug Delivery System Research, Sojo University, Ikeda 4-22-1, Kumamoto 860-0082; [3]Department of Pediatrics, Kumamoto Saishunsou National Hospital, 2659 Suya, Kohshi, Kumamoto 861-1196; [4]Division of Pediatrics, Department of Reproductive and Developmental Medicine, Faculty of Medicine, University of Miyazaki, Kiyotake-cho, Kihara 5200, Miyazaki 889-1692, Japan
Corresponding author: Hiroshi Maeda. Email: hirmaeda@ph.sojo-u.ac.jp

Abstract

Chronic granulomatous disease (CGD) causes impaired hydrogen peroxide (H_2O_2) generation. Consequently, neutrophils in patients with CGD fail to kill infecting pathogens. We expected that supplementation with H_2O_2 would effectively restore the bactericidal function of neutrophils in CGD. Here, we used polyethylene glycol-conjugated D-amino acid oxidase (PEG-DAO) as an H_2O_2 source. The enzyme DAO generates H_2O_2 by using D-amino acid and oxygen as substrates. PEG-DAO plus D-amino acid indeed exerted bacteriostatic activity against *Staphylococcus aureus* via H_2O_2 *in vitro*. Furthermore, use of PEG-DAO plus D-amino acids, which increased the amount of intracellular H_2O_2, restored bactericidal activity of neutrophils treated with diphenylene iodonium, in which nicotinamide adenine dinucleotide phosphate (NADPH) oxidase was defective. This restoration of bactericidal activity was mediated by myeloperoxidase, with concomitant production of H_2O_2 by PEG-DAO plus D-Ala. We also confirmed that PEG-DAO treatment restored bactericidal activity of congenitally defective neutrophils from patients with CGD. These results indicate that PEG-DAO can supply additional H_2O_2 for defective NADPH oxidase of neutrophils from patients with CGD, and thus neutrophils regain bactericidal activity.

Keywords: PEG-DAO, chronic granulomatous disease, hydrogen peroxide, H_2O_2 supplementation therapy

Experimental Biology and Medicine 2012; **00**: 1–6. DOI: 10.1258/ebm.2012.011360

Introduction

Chronic granulomatous disease (CGD) is a genetic disorder characterized by chronic and recurrent pyogenic infections. Patients with CGD have a defect in nicotinamide adenine dinucleotide phosphate (NADPH) oxidase that results in dysfunctional production of hydrogen peroxide (H_2O_2).[1,2] H_2O_2 plays a pivotal role in the antibacterial function of neutrophils, mediated by myeloperoxidase (MPO), so the impaired H_2O_2 production means failure of bactericidal activity against pathogenic organisms such as *Staphylococcus aureus*.[2,3]

D-Amino acid oxidase (DAO) is an enzyme containing flavin adenine dinucleotide (FAD).[4] The biochemical function of DAO involves oxidative deamination of D-amino acids, which yields the corresponding α-keto acids, a process in which molecular oxygen is used as an electron acceptor and H_2O_2 is generated.[5]

We previously prepared polyethylene glycol (PEG)-conjugated DAO (PEG-DAO), with comparable enzyme activity to native DAO.[6,7] More importantly, PEG-DAO had a longer circulation time in the blood, and preferential accumulation in inflamed sites, as a result of the enhanced permeability and retention (EPR) effect.[8,9] Our previous report showed that PEG-DAO exhibited selective cytotoxicity against various cancer cells via production of H_2O_2 *in vivo* and *in vitro*.[6,7]

We therefore anticipated that PEG-DAO would function as an alternative supplier of H_2O_2 for neutrophils in patients with CGD. In this study, we therefore investigated the effect of PEG-DAO on bactericidal activity of neutrophils from mice in which NADPH oxidase was inhibited, and from a patient with CGD, and analyzed the mechanism of bactericidal activity, in addition to investigating MPO-inhibited neutrophils.

Materials and methods

Materials

S. aureus strain ATCC25923 was used in these studies. ICR mice were purchased from Japan SLC, Inc., Shizuoka,

ISSN: 1535-3702

Japan. Trypticase soy (SCD) broth was purchased from Nissui Seiyaku Co., Tokyo, Japan. Flavin adenine dinucleotide was purchased from Sigma-Aldrich Chemical Co. (St Louis, MO, USA). Trypticase soy agar, isopropyl-β-D-thiogalactopyranoside, carbenicillin, Tween-20, ammonium sulfate, casein sodium salt and other reagents were from Wako Pure Chemical Industries, Ltd, Osaka, Japan. 4-aminobenzoic acid hydrazide (4-ABH) was from Merck KGaA, Frankfurt, Germany. Diphenylene iodonium (DPI) was purchased from Tokyo Chemical Industry Co., Ltd, Tokyo, Japan. Succinimide-activated PEG (MEC-50HS), with an average molecular size of Mr 5000, was purchased from Nippon Oil & Fat Co. (Tokyo, Japan).

Preparation of PEG-DAO

Recombinant porcine DAO was prepared as described previously.[7] Briefly, *Escherichia coli* BL21 (DE3) bacteria harboring the pET3c plasmid encoding porcine DAO were cultured in LB medium containing 50 μg/mL carbenicillin, and porcine DAO expression was achieved by adding 10 μmol/L isopropyl-β-D-thiogalactopyranoside to the medium with *E. coli*. After culture of the bacteria at 37°C for 20 h, bacterial pellets were sonicated (150 W, 30 min) in 17 mmol/L pyrophosphate buffer (pH 8.2) at 59°C, and porcine DAO was obtained by heat denaturation at 59°C for three minutes, followed by ammonium sulfate precipitation at 35% saturation, and then diethylaminoethyl cellulose column chromatography ($L = 10$ cm × $\phi = 1.6$ cm). The purity of DAO (>90%) was determined by using sodium dodecylsulfate polyacrylamide gel electrophoresis after staining with Coomassie brilliant blue. Pegylation of DAO was conducted as described previously.[6] In brief, to the DAO solution (2.0 mg/mL protein in 50 mmol/L sodium phosphate buffer, pH 7.4), succinimide-activated PEG was added at a 3.5 mol/L excess of PEG/mol of free amino groups in DAO and was allowed to react for one hour at 4°C. The reaction mixture containing PEG-DAO thus obtained was then purified to remove free PEG and other low-molecular-weight reactants by ultrafiltration with the YM-10 membrane (millipore) using 10 times the volume of 10 mmol/L phosphate-buffered saline (PBS). PEG-DAO was stored in PBS containing 0.1 mmol/L FAD at 4°C. Approximately 30% of amino group on DAO was reacted with PEG.

Bacteriostatic assay

S. aureus bacteria were cultured until the mid-log phase of growth in SCD broth with reciprocal shaking at 37°C. *S. aureus* bacteria were washed twice in saline and 1×10^6 CFU/mL of *S. aureus* were incubated with various concentrations of PEG-DAO, D-Ala, and with or without catalase in SCD broth at 37°C for five hours. The relative total numbers of bacteria were measured at turbidity at 570 nm and were correlated with the numbers of viable bacteria.

Preparation of neutrophils

Peritoneal neutrophils were elicited in 10-week-old female ICR mice by intraperitoneal injection of 3 mL per mouse of 6% casein sodium salt dissolved in physiological saline. At six hours after injection, neutrophils were harvested via peritoneal lavage with 5 mL of PBS, pH 7.4. Contaminating erythrocytes were removed by incubating in hypotonic saline solution (0.2% NaCl) for 30 s to cause erythrocytes to burst, after which isotonicity was restored via a rebalancing solution (1.9% NaCl) followed by centrifugation. Approximately 1×10^7 neutrophils were obtained from 10-week-old female ICR mice. The purity of the neutrophils (>90%) was checked by using Giemsa staining and examination of cell morphology with a conventional microscope (ECLIPSE TS100, Nikon). Human peripheral neutrophil was collected from a patient with CGD and a healthy volunteer using polymorphprep™ (Cosmo Bio) according to the manufacturer's instruction. Briefly, 5 mL of human blood sample was carefully layered on the top of 5 mL of Polymorphprep™, followed by centrifugation with a swing-out rotor for 30 min at 450 × *g*. The neutrophil fraction was collected and mixed with 0.45% NaCl, and then centrifuged for 10 min at 400 × *g*. Neutrophil pellets were then resuspended in PBS (−) and used for further experiments.

Bactericidal activity of neutrophils and preparation of CGDneutrophil mimics

Mouse peritoneal neutrophils were preincubated with 10 DPI or 10 μmol/L 4-ABH at 37°C for 15 min. *S. aureus*, which were cultured in SCD broth until the mid-log phase growth, were treated with 10% pooled mouse serum for effective neutrophilic endocytosis of *S. aureus*. Bacteria were added to neutrophils at the bacteria-to-neutrophil ratio of 10:1 (1×10^6 neutrophils/mL), and incubation proceeded at 37°C with reciprocal shaking at 0.5 Hz. After 30 min of incubation, non-phagocytosed bacteria were removed by swing-out centrifugation (at 110 × *g*, 4 min) and neutrophils were washed three times with PBS (+) containing 10 μmol/L DPI. Phagocytosed bacteria were precipitated with neutrophils, but non-phagocytosed bacteria were retained in the supernatant. Neutrophils that ingested the bacteria were incubated, at 37°C for 30 min with shaking, with increasing concentrations of PEG-DAO (10, 50 and 100 mU/mL) in the presence of 10 mmol/L D-Ala and PBS (+) containing 10 μmol/L DPI. Samples were diluted with 0.2% Tween-20, incubated at room temperature for five minutes to release phagocytosed bacteria, and vortexed vigorously, after which duplicate 100-μL aliquots were plated on 15 mL plates of SCD agar gel followed by overnight culture at 37°C. The numbers of viable bacteria were counted as described above.

Results

Bacteriostatic activity of PEG-DAO

We first examined the bacteriostatic activity of PEG-DAO against *S. aureus*. In the presence of 10 mmol/L D-Ala,